J|A|C|S
ARTICLES
Published on Web 02/20/2007

Alkenylsilane Structure Effects on Mononuclear and Binuclear Organotitanium-Mediated Ethylene Polymerization: Scope and Mechanism of Simultaneous Polyolefin Branch and Functional Group Introduction

Smruti B. Amin and Tobin J. Marks*

Contribution from the Department of Chemistry, Northwestern University, 2145 Sheridan Road, Evanston, Illinois 60208

Received October 20, 2006; E-mail: t-marks@northwestern.edu

Abstract: Alkenylsilanes of varying chain lengths are investigated as simultaneous chain-transfer agents and comonomers in organotitanium-mediated olefin polymerization processes. Ethylene polymerizations were carried out with activated $CGCTiMe_2$ and $EBICGCTi_2Me_4$ (CGC = $Me_2Si(Me_4C_5)(N^tBu)$; EBICGC = (μ-CH_2CH_2-3,3′){(η^5-indenyl)[1-$Me_2Si(^tBuN)$]}$_2$) precatalysts in the presence of allylsilane, 3-butenylsilane, 5-hexenylsilane, and 7-octenylsilane. In the presence of these alkenylsilanes, high polymerization activities (up to 10^7 g of polymer/(mol of Ti·atm ethylene·h)), narrow product copolymer polydispersities, and substantial amounts of long-chain branching are observed. Regardless of Ti nuclearity, alkenylsilane incorporation levels follow the trend $C_8H_{15}SiH_3 < C_6H_{11}SiH_3 \approx C_4H_7SiH_3 < C_3H_5SiH_3$. Alkenylsilane comonomer incorporation levels are consistently higher for $CGCTiMe_2$-mediated copolymerizations (up to 54%) in comparison with $EBICGCTi_2Me_4$-mediated copolymerizations (up to 32%). The long-chain branching levels as compared to the total branch content follow the trend $C_3H_5SiH_3 < C_4H_7SiH_3 \approx C_6H_{11}SiH_3 \approx C_8H_{15}SiH_3$, with gel permeation chromatography−multi-angle laser light scattering-derived branching ratios (g_M) approaching 1.0 for $C_8H_{15}SiH_3$. Time-dependent experiments indicate a linear increase of copolymer M_w with increasing polymerization reaction time. This process for producing long-chain branched polyolefins by coupling of an α-olefin with a chain-transfer agent in one comonomer is unprecedented. Under the conditions investigated, alkenylsilanes ranging from C_3 to C_8 are all efficient chain-transfer agents. Ti nuclearity significantly influences silanolytic chain-transfer processes, with the binuclear system exhibiting a sublinear relationship between M_n and [alkenylsilane]$^{-1}$ for allylsilane and 3-butenylsilane, and a superlinear relationship between M_n and [alkenylsilane]$^{-1}$ for 5-hexenylsilane and 7-octenylsilane. For the mononuclear Ti system, alkenylsilanes up to C_6 exhibit a linear relationship between M_n and [alkenylsilane]$^{-1}$, consistent with a simple silanolytic chain termination mechanism.

Introduction

Although polyolefins have an impressive range of important applications,[1] their ultimate efficacy is significantly constrained by the relative chemical inertness of these macromolecules. For example, this property leads to limited adhesion and compatibility with other materials as well as less than desired processability. These deficiencies could, in principle, be overcome by controlled introduction of reactive functionality and branches into the polymer backbone. Thus, functional groups and branching offer the potential to increase polyolefin melt-fracture resistance, paintability, elasticity, compatibility with other materials, and control of shear-thinning behavior.[2] Despite recent advances in homogeneous olefin polymerization catalysis,[1] controlling polymer microstructure still remains a challenge. One approach to controlling polymer microstructure is by manipulating specific polymerization chain termination pathways. Chain-transfer agents, defined as reagents which both terminate and facilitate reinitiation of a growing polymer chain, can efficiently control molecular weight and simultaneously

(1) Recent reviews on olefin polymerization and copolymerization: (a) Marks, T. J., Ed. *Proc. Natl. Acad. Sci. U.S.A.* **2006**, *103*, 15288−15354 and contributions therein (special feature on "Polymerization"). (b) Gibson, V. C.; Spitzmesser, S. K. *Chem. Rev.* **2003**, *103*, 283. (c) Pedeutour, J.-N.; Radhakrishnan, K.; Cramail, H.; Deffieux, A. *Macromol. Rapid Commun.* **2001**, *22*, 1095. (d) Chen, Y.-X.; Marks, T. J. *Chem. Rev.* **2000**, *100*, 1391. (e) Gladysz, J. A., Ed. *Chem. Rev.* **2000**, *100* (special issue on "Frontiers in Metal-Catalyzed Polymerization"). (f) Marks, T. J., Stevens, J. C., Eds. *Top. Catal.* **1999**, *7*, and references therein. (g) Jordan, R. F., Ed. *J. Mol. Catal.* **1998**, *128*, and references therein. (h) Kaminsky, W.; Arndt, M. *Adv. Polym. Sci.* **1997**, *127*, 144−187. (i) Bochmann, M. J. *J. Chem. Soc., Dalton Trans.* **1996**, 255−270 and references therein. (j) Brintzinger, H.-H.; Fisher, D.; Mülhaupt, R.; Rieger, B.; Waymouth, R. M. *Angew. Chem., Int. Ed. Engl.* **1995**, *34*, 1143−1170. (k) Simonazzi, T.; Nicola, A.; Aglietto, M.; Ruggeri, G. In *Comprehensive Polymer Science*; Allen, G., Aggarwal, S. L., Russo, S., Eds.; Pergamon Press: Oxford, 1992; First Supplement, Chapter 7.

(2) Effects of functional groups and branching on polyolefin properties: (a) Chung, T. C. *Prog. Polym. Sci.* **2002**, *27*, 39. (b) Imuta, J.-I.; Kashiwa, N.; Toda, Y. *J. Am. Chem. Soc.* **2002**, *124*, 1176. (c) Dong, J. Y.; Wang, Z.; Hong, H.; Chung, T. C. *Macromolecules* **2002**, *35*, 9352. (d) Chung, T. C. *Polym. Mater. Sci. Eng.* **2001**, *84*, 33. (e) Chum, P. S.; Kruper, W. J.; Guest, M. J. *Adv. Mater.* **2000**, *12*, 1759. (f) Alt, H. G.; Föttinger, K.; Milius, W. J. *Organomet. Chem.* **1999**, *572*, 21. (g) Harrison, D.; Coulter, I. M.; Wang, S. T.; Nistala, S.; Kuntz, B. A.; Pigeon, M.; Tian, J.; Collins, S. *J. Mol. Catal. A: Chem.* **1998**, *128*, 65. (h) Nesarikar, A. R.; Carr, S. H.; Khait, K.; Mirabella, F. M. *J. Appl. Polym. Sci.* **1997**, *63*, 1179.

10.1021/ja0675292 CCC: $37.00

Scheme 1. Proposed Catalytic Cycle for Organotitanium-Mediated Ethylene Polymerization in the Presence of Electron-Deficient Chain-Transfer Agents[a]

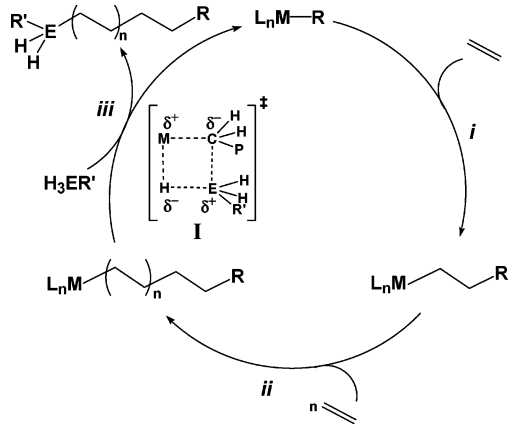

[a] P = polymer chain; E - Si, B, Al; R = alkyl, H; R′ = alkyl, aryl.

introduce functionality at macromolecule chain ends.[3−8] A priori, introducing such functionality in concert with the polymerization process is preferred over post-polymerization modification, which can be difficult due to the unreactive nature of hydrocarbon polymers and the lack of control in both macromolecule functionality levels and locations. To date, strategies to introduce comonomers that have the capacity to undergo rapid insertion (chain propagation) as well as to effect reactive functionality-introducing chain-transfer processes have not, to our knowledge, been explored.[9]

Organotitanium complexes are among the most versatile catalysts for single-site Ziegler−Natta-type α-olefin polymerization.[10] Organotitanium catalysts such as $Me_2Si(Me_4C_5)(N^tBu)TiMe_2$ (CGCTiMe$_2$, **1**), in combination with appropriate activators/cocatalysts, are known to effect the polymerization of various α-olefins with activities as large as 10^7 g/(mol of Ti·h·atm ethylene) and to afford high molecular weight polymers with narrow polydispersities. These "CGC" catalysts produce polyethylene containing long-chain branches (LCBs) under circumstances in which vinyl-terminated, chain-transferred macromolecules have an elevated probability of re-enchainment into the growing polymer chain at a second catalyst center.[2] The resulting small but significant levels of long-chain branching, where we define a LCB as a polymeric branch, lead to extremely advantageous materials properties.[2] In addition, such titanium catalysts can efficiently polymerize and copolymerize sterically encumbered comonomers that have traditionally been difficult to enchain.[11,12] Polynuclear organotitanium catalysts, such as $(\mu\text{-}CH_2CH_2\text{-}3,3')\{(\eta^5\text{-indenyl})[1\text{-}Me_2Si(^tBuN)]\}_2Ti_2Me_4$ (EBICGCTi$_2$Me$_4$, **2**), also afford high molecular weight polyolefins with dramatically enhanced α-olefin comonomer incorporation versus mononuclear analogues.[12] The dicationic bimetallic framework likely exhibits enhanced binding affinity (e.g., **3**), resulting in enhanced comonomer enchainment.

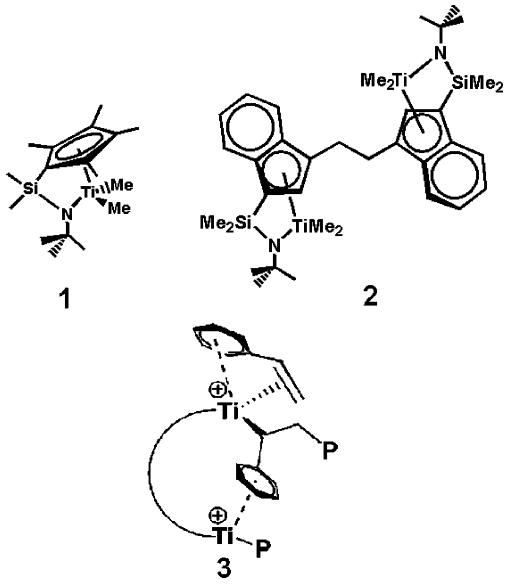

In addition to these interesting characteristics, many single-site organotitanium catalysts exhibit high activity for silanolytic chain transfer,[4b] a process which efficiently introduces organosilane functionality into polyolefin chains (Scheme 1). These observations raise the intriguing question of whether the two types of transformations could be coupled by introducing unsaturated alkenylsilanes as comonomers into a single-site

(3) Organoaluminum chain transfer: (a) Götz, C.; Rau, A.; Luft, G. *Macromol. Mater. Eng.* **2002**, *287*, 16. (b) Kukral, J.; Lehmus, P.; Klinga, M.; Leskelä, M.; Rieger, B. *Eur. J. Inorg. Chem.* **2002**, 1349. (c) Han, C. J.; Lee, M. S.; Byun, D.-J.; Kim, S. Y. *Macromolecules* **2002**, *35*, 8923. (d) Liu, J.; Støvneng, J. A.; Rytter, E. *J. Polym. Sci., Part A: Polym. Chem.* **2001**, *39*, 3566.

(4) Silane chain transfer: (a) Amin, S. B.; Marks, T. J. *J. Am. Chem. Soc.* **2006**, *128*, 4506. (b) Koo, K.; Marks, T. J. *J. Am. Chem. Soc.* **1999**, *121*, 8791. (c) Koo, K.; Fu, P.-F.; Marks, T. J. *Macromolecules* **1999**, *32*, 981. (d) Koo, K.; Marks, T. J. *Chemtech* **1999**, *29* (10), 13. (e) Fu, P.-F.; Marks, T. J. *J. Am. Chem. Soc.* **1995**, *117*, 10747.

(5) Borane chain transfer: (a) Dong, J. Y.; Wang, Z. M.; Hong, H.; Chung, T. C. *Macromolecules* **2002**, *35*, 9352. (b) Dong, J. Y.; Chung, T. C. *Macromolecules* **2002**, *35*, 1622. (c) Dong, J. Y.; Manias, E.; Chung, T. C. *Macromolecules* **2002**, *35*, 3430. (d) Chung, T. C.; Dong, J. Y. *J. Am. Chem. Soc.* **2001**, *123*, 4871.

(6) Thiophene chain transfer: Ringelberg, S. N.; Meetsma, A.; Hessen, B.; Teuben, J. H. *J. Am. Chem. Soc.* **1999**, *121*, 6082.

(7) Phosphine chain transfer: (a) Kawaoka, A. M.; Marks, T. J. *J. Am. Chem. Soc.* **2005**, *127*, 6311. (b) Kawaoka, A. M.; Marks, T. J. *J. Am. Chem. Soc.* **2004**, *126*, 12764.

(8) Organozinc chain transfer: (a) Arriola, D. J.; Carnahan, E. M.; Hustad, P. D.; Kuhlman, R. L.; Wenzel, T. T. *Science* **2006**, *312*, 714. (b) van Meurs, M.; Britovsek, G. J. P.; Gibson, V. C.; Cohen, S. A. *J. Am. Chem. Soc.* **2005**, *127*, 9913 and references therein.

(9) For representative patent literature regarding olefin/alkenylsilane polymerization, see: (a) Arriola, D. J.; Bishop, M. T.; Campbell, R. E.; Devore, D. D.; Hahn, S. E.; Ho, T. H.; McKeand, T. J.; Timmers, F. J. (Dow Chemical Co.). U.S. Patent Application US 234831, 2003. (b) Sugimoto, R.; Ishii, Y.; Kawanishi, K.; Nishimori, Y.; Inoe, N.; Asanuma, T. (Mitsui Toatsu Chemical Co.). Japan Patent Application JP 0830281, 1996. (c) Montecatini Chemical Co. U.S. Patent Application US 3644306, 1969.

(10) (a) Okuda, J. *Dalton Trans.* **2003**, *12*, 2367. (b) Metz, M. V.; Sun, Y.; Stern, C. L.; Marks, T. J. *Organometallics* **2002**, *21*, 3691. (c) McKnight, A. L.; Waymouth, R. M. *Chem. Rev.* **1998**, *98*, 2587. (d) Chen, Y.-X.; Marks, T. J. *Organometallics* **1997**, *16*, 3649. (e) Stevens, J. C.; Timmers, F. J.; Wilson, D. R.; Schmidt, G. F.; Nickias, P. N.; Rosen, R. K.; Knight, G. W.; Lai, S. (Dow Chemical Co.). European Patent Application EP 0416815 A2, 1991; *Chem. Abstr.* **1991**, *115*, 93163.

(11) Mononuclear organotitanium-mediated polymerization of functionalized and sterically hindered monomers: (a) Yoon, J.; Mathers, R. T.; Coates, G. W.; Thomas, E. L. *Macromolecules* **2006**, *39*, 1913. (b) Gendler, S.; Groysman, S.; Goldschmidt, Z.; Shuster, M.; Kol, M. *J. Polym. Sci., Part A: Polym. Chem.* **2006**, *44*, 1136. (c) Furuyama, R.; Mitani, M.; Mohri, J.-I.; Mori, R.; Tanaka, H.; Fujita, T. *Macromolecules* **2005**, *38*, 1546. (d) Tang, L.-M.; Hu, T.; Pan, L.; Li, Y.-S. *J. Polym. Sci., Part A: Polym. Chem.* **2005**, *43*, 6323. (e) Jensen, T. R.; O'Donnell, J. J., III; Marks, T. J. *Organometallics* **2004**, *23*, 740. (f) Jensen, T. R.; Yoon, S. C.; Dash, A. K.; Luo, L.; Marks, T. J. *J. Am. Chem. Soc.* **2003**, *125*, 14482. (g) Chien, J. C. W.; Yu, Z.; Marques, M. M.; Flores, J. C.; Rausch, M. D. *J. Polym. Sci., Part A: Polym. Chem.* **1998**, *36*, 319. (h) Sernetz, F. G.; Mülhaupt, R. *J. Polym. Sci., Part A: Polym. Chem.* **1997**, *35*, 2549. (i) Patten, T. E.; Novak, B. M. *J. Am. Chem. Soc.* **1996**, *118*, 1906.

(12) Polynuclear organo-group 4-mediated polymerization of functionalized and sterically hindered monomers: (a) Li, H.; Marks, T. J. In ref 1a, p 15295. (b) Li, H.; Li, L.; Schwartz, D. J.; Metz, M. V.; Marks, T. J.; Liable-Sands, L.; Rheingold, A. L. *J. Am. Chem. Soc.* **2005**, *127*, 14756. (c) Guo, N.; Li, L.; Marks, T. J. *J. Am. Chem. Soc.* **2004**, *126*, 6542. (d) Li, H.; Li, L.; Marks, T. J.; Liable-Sands, L.; Rheingold, A. L. *J. Am. Chem. Soc.* **2003**, *125*, 10788. (e) Abramo, G. P.; Li, L.; Marks, T. J. *J. Am. Chem. Soc.* **2002**, *124*, 13966.

Scheme 2. Proposed Catalytic Cycle for Organotitanium-Mediated Alkenylsilane/Ethylene Copolymerization

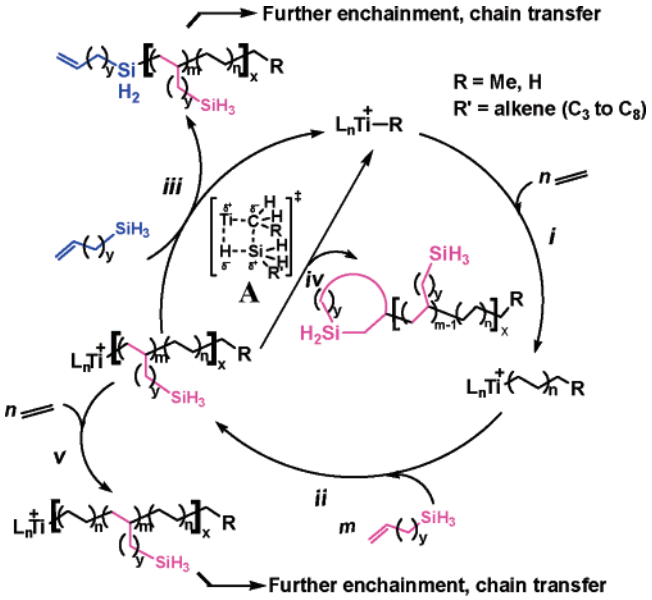

olefin polymerization cycle, i.e., Scheme 2. For electron-deficient chain-transfer agents such as alanes,[3] silanes,[4] and boranes,[5] the heteroatom is delivered to the polymer chain terminus at the end of each polymerization cycle as the final C-heteroatom bond-forming step (Scheme 1, step *iii*), and delivery is proposed to occur via four-centered σ-bond metathesis transition state **I** in Scheme 1.

We previously reported[4b] that silane-capped polyolefins can be produced efficiently in the presence of $PhSiH_3$ via an organotitanium-mediated catalytic cycle (Scheme 1; E = Si, R′ = Ph). It was demonstrated that polymer molecular weight can be modulated by varying the silane concentration and that the silyl group is selectively transferred to the polymer chain end in a process that is regiochemically distinct from that expected in a simple catalytic hydrosilylation.[4] Although organotitanium catalysts effectively mediate silanolytic chain transfer for many olefin polymerization processes, they are conspicuously inefficient in ethylene polymerization, for reasons not entirely understood.[4b] Thus, silanes containing α-olefinic functionality offer the intriguing potential of poising reactive groups in closer proximity to the Ti−C bond to afford silane-capped, branched polyethylenes, all employing a single reagent/comonomer. If efficient, this process would provide an approach to simultaneously introducing both chain branching and a versatile reactive functionality[13] into polyolefin architectures. The proposed catalytic cycle for this synthesis of silane-capped ethylene/alkenylsilane copolymers (Scheme 2) is envisioned to proceed via sequences of (i),(v) multiple insertions of C=C unsaturation into Ti−alkyl bonds, (ii) C=C insertion of the alkenylsilane into the growing polymer chain, and/or (iii) *inter*molecular silanolytic chain transfer to the copolymer chain, and/or (iv) *intra*molecular silanolytic chain transfer to the copolymer chain, to complete the cycle.[4a]

(13) Organosilanes in organic synthesis: (a) *Comprehensive Organic Functional Group Transformations II*; Katritzky, A. R., Taylor, R. J., Eds.; Elsevier: Boston, 2005; Vols. 1, 2, 4, and 5. (b) *Comprehensive Organic Functional Group Transformations*; Katritzky, A. R., Meth-Cohn, O., Rees, C. W., Eds.; Pergamon Press: New York, 1995; Vols. 1−5. (c) *Comprehensive Organic Synthesis*; Trost, B. M., Fleming, I., Eds.; Pergamon Press: New York, 1991; Vols. 2, 6, and 8. (d) Thomas, S. E. *Organic Synthesis: The Roles of Boron and Silicon*; Oxford University Press: New York, 1991. (e) Colvin, E. *Silicon in Organic Synthesis*; Butterworth and Co. Ltd.: Boston, 1981.

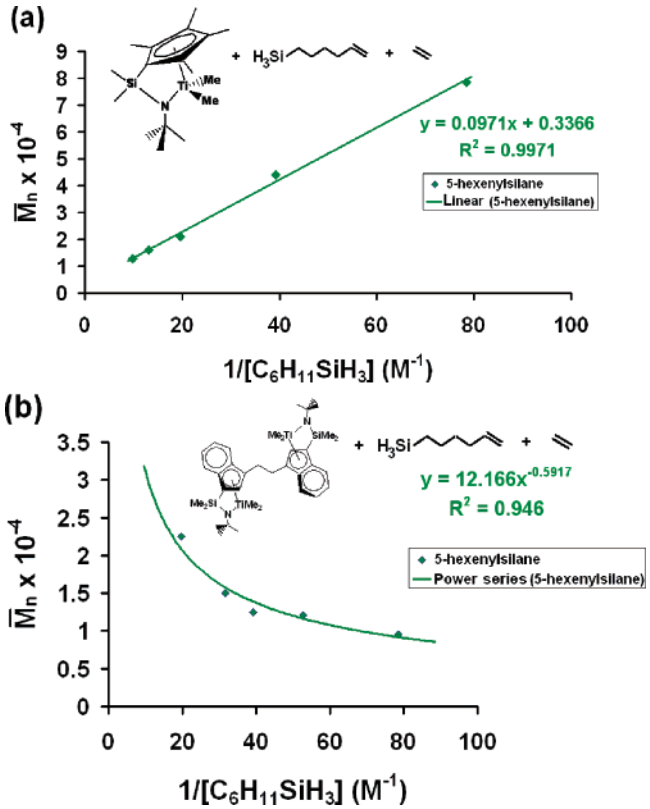

Figure 1. Relationship of ethylene + 5-hexenylsilane copolymer number-average molecular weight (GPC vs polyethylene standards) to inverse 5-hexenylsilane concentration at fixed ethylene and (a) $CGCTiMe_2$ and (b) $EBICGCTi_2Me_4$ concentrations.

In a preliminary investigation, it was communicated that organotitanium-mediated ethylene/5-hexenylsilane copolymerizations yield 5-hexenylsilane-capped ethylene/5-hexenylsilane copolymers, demonstrating that coupling of insertion and chain-transfer chemistry using a single comonomer is, in fact, an efficient process.[4a] In the present contribution, we expand the scope of this exploratory study to include a wider range of organotitanium catalysts of varying nuclearity as well as a series of alkenylsilane reagents of sequentially varied architecture in order to more fully investigate the scope of this organotitanium-mediated copolymer synthesis. In addition, we present a full discussion of the polymerization scope, kinetics, and mechanism involving such a dual-purpose comonomer, focusing on the effect of alkenylsilane chain length and titanium nuclearity on the course and relative efficiency of the insertion and chain-transfer processes. It will be seen that, by manipulating alkenylsilane chain length and Ti nuclearity, a large diversity of polyethylene architectures can be synthesized in a controlled polymerization system.

Experimental details are presented in the Supporting Information.

Results

The aim of this research was to investigate the scope and mechanism of alkenylsilanes as bifunctional comonomers for organotitanium-mediated olefin polymerizations. Previously, we communicated the catalytic synthesis of 5-hexenylsilane/ethyl-

ene copolymers.[4a] In this contribution, we extend the study to include both mononuclear and binuclear organotitanium catalyst-mediated polymerizations (i.e., **1**, **2**) and systematically expand the comonomer scope to include α,ω-alkenylsilanes ranging from C_3 to C_8 (**4**). After a concise discussion of catalyst

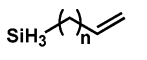

n = 1, 2, 4, 6

4

activation and M−C/Si−H transposition chemistry, we discuss the relative chain-transfer efficiencies of allyl-, 3-butenyl-, 5-hexenyl-, and 7-octenylsilane. Next, the effects of alkenylsilane chain length and Ti catalyst nuclearity on polymer microstructure will be addressed from a mechanistic standpoint. Finally, mechanistic precedent in α-olefin copolymerizations and silanolytic chain transfer will be used to understand the observed trends in reactivity and polyolefin microstructure.

Catalyst Activation and M−C/Si−H Transposition. The reaction between the precatalyst $CGCTiMe_2$ and the cocatalyst $Ph_3C^+B(C_6F_5)_4^-$ produces the catalytically active ion-paired species $CGCTiMe^+B(C_6F_5)_4^-$ (eq 1).[14] The catalyst $CGCTiMe^+B(C_6F_5)_4^-$ has a relatively open coordination sphere due to the "constrained geometry" ancillary ligand system. Similar to a variety of other organoborane/organoborate cocatalysts,[1d,15] the weakly coordinating $B(C_6F_5)_4^-$ anion[1d,15a,16] plays a significant role in enhancing the olefin polymerization activity, affording

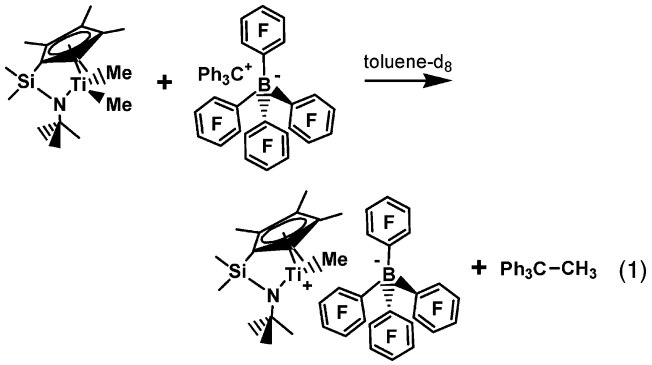

(1)

productivities as high as 10^7 g/(mol of Ti·atm ethylene·h) at 25 °C when paired with $CGCTiMe_2$. Preliminary screens for stoichiometric M−C/Si−H transposition activity were performed by contacting $CGCTiMe^+B(C_6F_5)_4^-$ with $C_6H_{13}SiH_3$ in toluene-d_8. As monitored in situ by ^{1}H NMR, rapid Ti−C/Si−H transposition occurs at room temperature, yielding $(C_6H_{13})(Me)SiH_2$ and what is presumably a cationic organotitanium hydride (eq 2).[1c,17]

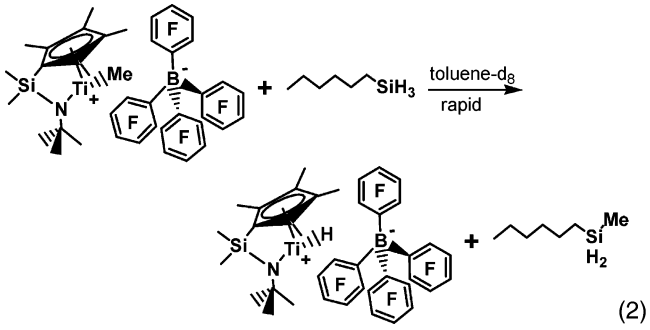

(2)

These observations next motivated further investigations into the reactivity of 5-hexenylsilane with respect to rapid, repetitive insertion (propagation) at a single-site olefin polymerization center. Preliminary test polymerizations of $C_6H_{11}SiH_3$ mediated by $CGCTiMe^+B(C_6F_5)_4^-$ were carried out in toluene-d_8. As monitored in situ by ^{1}H NMR, rapid insertion of 5-hexenylsilane into the Ti−alkyl bond occurs to produce oligomeric materials containing $n = 5$ to $n = 9$ monomer units based on EI mass spectrometry (eq 3). ^{13}C NMR resonances of the oligomers

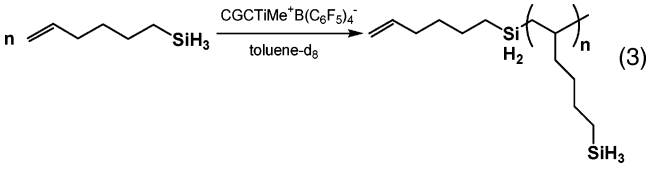

(3)

indicate butyl branches, each terminated with a single silyl group, by comparison to literature data for 1-hexene homopolymers.[18] The ^{1}H NMR spectrum exhibits resonances at δ 3.7 and δ 3.9, which is consistent with the presence of SiH_3 and SiH_2 groups, respectively.[4] All of these preliminary observations motivated the detailed investigation of alkenylsilane effects on single-site, organotitanium-catalyzed olefin polymerization discussed below.

Chain-Transfer Efficiency of 5-Hexenylsilane in Organotitanium-Mediated Ethylene Copolymerizations. Polymeric Products, Nuclearity Effects, and Comparison to *n*-Hexylsilane. The first alkenylsilane investigated as a chain-transfer agent/comonomer for organotitanium-mediated ethylene polymerization was 5-hexenylsilane (Table 1). All polymerizations were performed under 1.0 atm ethylene pressure and rigorously anaerobic/anhydrous conditions using procedures minimizing

(14) Catalyst activation: (a) Song, F.; Lancaster, S. J.; Cannon, R. D.; Schormann, M.; Humphrey, S. M.; Zuccaccia, C.; Macchioni, A.; Bochmann, M. *Organometallics* **2005**, *24*, 1315. (b) Zuccaccia, C.; Stahl, N. G.; Macchioni, A.; Chen, M.-C.; Roberts, J. A. S.; Marks, T. J. *J. Am. Chem. Soc.* **2004**, *126*, 1448. (c) Hollink, E.; Wei, P.; Stephan, D. W. *Organometallics* **2004**, *23*, 1562. (d) Song, F.; Cannon, R. D.; Lancaster, S. J.; Bochmann, M. *J. Mol. Catal. A: Chemical* **2004**, *218*, 21. (e) Stahl, N. G.; Zuccaccia, C.; Jensen, T. R.; Marks, T. J. *J. Am. Chem. Soc.* **2003**, *125*, 5256. (f) Metz, M. V.; Sun, Y.; Stern, C. L.; Marks, T. J. *Organometallics* **2002**, *21*, 3691.

(15) Organoboranes as cocatalysts: (a) Chen, M.-C.; Roberts, J. A. S.; Marks, T. J. *J. Am. Chem. Soc.* **2004**, *126*, 4605. (b) Metz, M. V.; Schwartz, D. J.; Stern, C. L.; Marks, T. J.; Nickias, P. N. *Organometallics* **2002**, *21*, 4159. (c) Lanza, G.; Fragala, I. L.; Marks, T. J. *Organometallics* **2002**, *21*, 5594. (d) Lanza, G.; Fragala, I. L.; Marks, T. J. *Organometallics* **2001**, *20*, 4006. (e) Lanza, G.; Fragala, I. L.; Marks, T. J. *J. Am. Chem. Soc.* **2000**, *122*, 12764. (f) Chase, P. A.; Piers, W. E.; Patrick, B. O. *J. Am. Chem. Soc.* **2000**, *122*, 12911. (g) Piers, W. E.; Irvine, G. J.; Williams, V. C. *Eur. J. Inorg. Chem.* **2000**, *10*, 2131. (h) Williams, V. C.; Piers, W. E.; Clegg, W.; Elsegood, M. R. J.; Collins, S.; Marder, T. B. *J. Am. Chem. Soc.* **1999**, *121*, 3244. (i) Chen, Y.-X.; Metz, M. V.; Li, L.; Stern, C. L.; Marks, T. J. *J. Am. Chem. Soc.* **1998**, *120*, 6287. (j) Li, L.; Marks, T. J. *Organometallics* **1998**, *17*, 3996.

(16) Weakly coordinating anions: (a) Chen, M.-C.; Roberts, J. A. S.; Seyam, A. M.; Li, L.; Zuccaccia, C.; Stahl, N. G.; Marks, T. J. *Organometallics* **2006**, *25*, 2833. (b) Chen, M.-C.; Roberts, J. A. S.; Marks, T. J. *Organometallics* **2004**, *23*, 932. (c) Juhasz, M.; Hoffmann, S.; Stoyanov, E,; Kim, K.-C.; Reed, C. A. *Angew. Chem., Int. Ed.* **2004**, *43*, 5352. (d) Reed, C. A. *Acc. Chem. Res.* **1998**, *31*, 133.

(17) M−C/Si−H transposition: (a) Jia, L.; Zhao, J.; Ding, E.; Brennessel, W. W. *J. Chem. Soc., Dalton Trans.* **2002**, *13*, 2608. (b) Gauvin, F.; Harrod, J. F. *Adv. Organomet. Chem.* **1998**, *42*, 363. (c) King, W. A.; Marks, T. J. *Inorg. Chim. Acta* **1995**, *229*, 343. (d) Fu, P.-F.; Brard, L.; Li, Y.; Marks, T. J. *J. Am. Chem. Soc.* **1995**, *117*, 7157. (e) Yang, X.; Jia, L.; Marks, T. J. *J. Am. Chem. Soc.* **1993**, *115*, 3392. (f) Forsyth, C. M.; Nolan, S. P.; Marks, T. J. *Organometallics* **1991**, *10*, 2543.

(18) (a) Henschke, O.; Knorr, J.; Arnold, M. *J. Macromol. Sci. Chem.* **1998**, *A35*, 473. (b) Babu, G.; Newmark, R. *Macromolecules* **1994**, *27*, 3383.

Table 1. Organotitanium-Catalyzed Ethylene Polymerization in the Presence of 5-Hexenylsilane

entry	precatalyst[a,b]	[precatalyst] (μM)	[$C_6H_{11}SiH_3$] (mM)	activity[c] ($\times 10^4$)	M_n[d]	M_w/M_n[d]	T (°C)	T_m (°C)	comonomer incorporation (%)[e]
1	Cp*$TiMe_3$	200	102	7.10	4 600	2.4	23	112	6.0
2	CGC$TiMe_2$	200	12.8	500	78 600	2.4	26	126	1.0
3	CGC$TiMe_2$	200	25.5	290	43 900	2.6	24	125	1.0
4	CGC$TiMe_2$	200	51.1	4.70	21 100	3.7	29	126	2.0
5	CGC$TiMe_2$	200	76.5	0.09	15 900	3.3	22	126	3.0
6	CGC$TiMe_2$	200	102	0.06	12 700	2.6	23	124	3.0
7	EBICGCTi_2Me_4	100	12.8	180	9 600	2.4	30	105	1.0
8	EBICGCTi_2Me_4	100	19.0	6.00	12 100	2.2	25	103	1.0
9	EBICGCTi_2Me_4	100	25.5	1.31	12 500	2.3	24	103	2.0
10	EBICGCTi_2Me_4	100	31.6	1.43	15 000	2.4	25	106	2.0
11	EBICGCTi_2Me_4	100	51.1	0.11	22 500	1.7	25	105	2.0

[a] CGC = $Me_2Si(Me_4C_5)(N^tBu)$, EBI = ethylene-bridged bis(indenyl). Polymerization conditions: 50 mL of toluene, 2.0 min for entries 1−6, 10 min for entries 7−11. [b] Cocatalyst = 10 μmol of $Ph_3CB(C_6F_5)_4$. [c] Units = g/(mol of Ti·h·atm ethylene). [d] By GPC in 1,2,4-trichlorobenzene vs polyethylene standards. [e] Comonomer incorporation calculated on the basis of ^{13}C NMR spectra.

mass transport effects,[19] with the olefin concentration held constant and the 5-hexenylsilane concentration maintained in pseudo-zero-order excess. The ^1H and ^{13}C NMR spectra of the silane-terminated ethylene/5-hexenylsilane copolymers exhibit characteristic proton butylsilane branch (δ 0.25, 0.70, 2.2, 3.6), polyethylene backbone (δ 1.0−1.5), and $-CH_3$ chain end (δ 0.98) resonances (Figure S1).[4,7,18] In addition, the ^{13}C NMR and gel permeation chromatography−multi-angle laser light scattering (GPC-MALLS) data indicate approximately 40 butylsilane branches per 1000 carbons. The concentrations of any vinyl chain end resonances in these materials are below the detection limits in both the ^1H and ^{13}C NMR spectra, suggesting that chain termination via β-hydride elimination (to metal center or monomer)[20] is inconsequential. Furthermore, the ~3:1 $-CH_2$-SiH_3:$-CH_2SiH_2$ ^{13}C NMR intensity ratio suggests that 5-hexenylsilane readily undergoes insertion into the polymer chain and silanolytically effects inter- and/or intramolecular chain termination, thereby functionalizing the polymer chain end. The $-\boldsymbol{C}H_2-$ resonances from cyclized end groups directly overlap with the main $-\boldsymbol{C}H_2-$ polymer backbone resonance; thus, the amount of cyclized end groups cannot be quantified. In addition, the $-SiH_2-$ resonances in both the ^1H and ^{29}Si NMR spectra for cyclic vs acyclic end groups cannot be distinguished from one another, as verified by NMR spectroscopy on small-molecule analogues (all of the ^1H NMR resonances are at ~4.0 ppm, and ^{29}Si NMR resonances are at ~ −24 ppm). In addition, the resulting 5-hexenylsilane-capped copolymers have relatively narrow, monomodal polydispersities (Table 1), consistent with a single-site process.

For polymerizations conducted in the presence of 5-hexenylsilane, titanium nuclearity and polymer molecular weight are inversely related. Thus, ethylene/5-hexenylsilane polymerizations mediated by binuclear EBICGCTi_2Me_4/2$Ph_3C^+B(C_6F_5)_4^-$ require long reaction times (as compared to mononuclear organotitanium catalysts) to produce significant amounts of polymer having lower molecular weight (M_n = 12 500; Table 1, entry 9). In contrast, CGC$TiMe_2$/$Ph_3C^+B(C_6F_5)_4^-$-mediated polymerizations result in copolymers with higher molecular weight (M_n = 43 900; Table 1, entry 3), produced with considerably higher activities (10^6 g of polymer/(mol of Ti·atm ethylene·h)). The EBICGCTi_2Me_4/2$Ph_3C^+B(C_6F_5)_4^-$ active catalyst is deep reddish-brown and maintains this color throughout the polymerization, suggesting the presence of a stable active species.[12c] The CGC$TiMe_2$/$Ph_3C^+B(C_6F_5)_4^-$ active catalyst is bright orange and maintains this color throughout the polymerization, again suggesting the presence of a stable active species.[15j] In addition, at constant catalyst and ethylene concentrations, product copolymer molecular weight scales inversely with silane concentration for CGC$TiMe_2$ (Table 1, entries 2−6; Figure 1a), supporting the chain-transfer mechanism shown in Scheme 2 (eq 7, vide infra). Interestingly, under similar conditions, product copolymer molecular weight *increases* as an approximate superlinear series with increasing silane concentration for EBICGCTi_2Me_4, supporting the mechanism for further enchainment and chain-transfer processes shown in Scheme 2, steps ii and v (Table 1, entries 7−11; Figure 1b). Further mechanistic insights will be offered in the Discussion section below.

To better understand the role of the olefinic moiety in 5-hexenylsilane copolymerizations, a series of control ethylene polymerizations was performed in the presence of *n*-hexylsilane (Table 2). Note that here the chain-transfer plot for *n*-hexylsilane in place of 5-hexenylsilane (Figure 2b) has a near-zero slope, indicating that *n*-hexylsilane functions as a *highly inefficient* chain-transfer agent. In addition, the product ^1H NMR resonances at δ 5.0 and δ 5.5 indicate the presence of vinylic end groups in the polymer microstructure.

Chain-Transfer Efficiency of Allylsilane in Organotitanium-Mediated Ethylene Copolymerizations. Allylsilane was also investigated as a comonomer/chain-transfer agent for ethylene polymerization using organotitanium catalysts (Table 3). The ^1H, ^{13}C, and ^{29}Si NMR spectra of the silane-terminated ethylene/allylsilane copolymers exhibit characteristic proton methylsilane branch (δ 0.88, 1.60, 3.58), polyethylene backbone (δ 1.2−1.5), and $-CH_3$ chain end (δ 0.96) resonances (Figure S2). The concentration of vinyl chain end resonances is very small in the ^1H NMR spectrum, indicating that chain transfer via β-hydride elimination is insignificant and that allylsilane chain termination is the dominant chain-transfer pathway. Furthermore, the intense $-SiH_3$ resonance in the ^1H and ^{29}Si NMR spectra suggests that allylsilane readily undergoes insertion into the polymer chain in addition to effecting chain transfer at the polymer chain end. In addition, the resulting allylsilane-capped copolymers have narrow, monomodal polydispersities,

(19) Jeske, G.; Lauke, H.; Mauermann, H.; Swepston, P. N.; Schumann, H.; Marks, T. J. *J. Am. Chem. Soc.* **1985**, *107*, 8091.
(20) Chain-transfer pathways in olefin polymerization: (a) Talarico, G.; Budzelaar, P. H. M. *J. Am. Chem. Soc.* **2006**, *128*, 4524 and references therein. (b) Resconi, L.; Cavallo, L.; Fait, A.; Piemontesi, F. *Chem. Rev.* **2000**, *100*, 1253 and references therein.

Table 2. Organotitanium-Catalyzed Ethylene Polymerization in the Presence of *n*-Hexylsilane

entry	precatalyst[a,b]	[precatalyst] (μM)	[$C_6H_{13}SiH_3$] (mM)	activity[c] ($\times 10^4$)	M_n[d]	M_w/M_n[d]	T (°C)	T_m (°C)
1	$CGCTiMe_2$	200	24.9	950	34 900	2.7	32	144
2	$CGCTiMe_2$	200	49.7	1100	32 000	3.0	28	144
3	$CGCTiMe_2$	200	74.6	900	33 500	2.8	33	143
4	$CGCTiMe_2$	200	99.4	850	28 400	3.3	34	142
5	$CGCTiMe_2$	200	122	1000	35 300	2.1	34	144
6	$CGCTiMe_2$	200	245	300	36 600	2.8	33	141
7	$CGCTiMe_2$	200	367	100	38 700	3.0	28	144
8	$CGCTiMe_2$	200	490	40	33 800	2.9	26	144

[a] CGC = $Me_2Si(Me_4C_5)(N^tBu)$, EBI = ethylene-bridged bis(indenyl). Polymerization conditions: 50 mL of toluene, 2.0 min. [b] Cocatalyst = 10 μmol of $Ph_3CB(C_6F_5)_4$. [c] Units = g/(mol of Ti·h·atm ethylene). [d] By GPC in 1,2,4-trichlorobenzene vs polyethylene standards

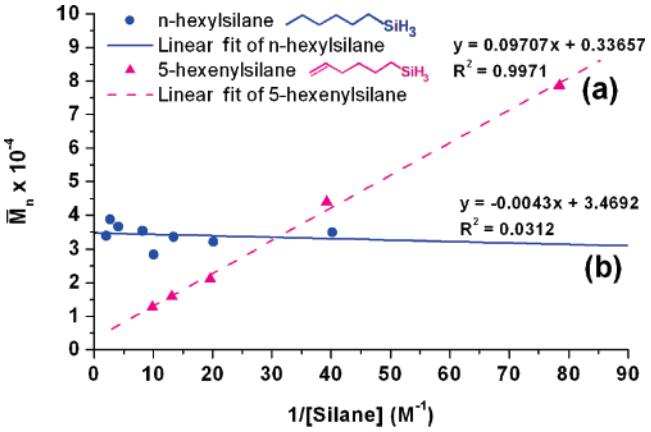

Figure 2. Relationship of polyethylene number-average molecular weight (GPC versus polyethylene) to (a) inverse $C_6H_{11}SiH_3$ concentration at fixed catalyst and ethylene concentrations and (b) inverse *n*-$C_6H_{13}SiH_3$ concentration at fixed catalyst and ethylene concentrations.

consistent with a single-site polymerization process, and a strong ^{29}Si NMR resonance at δ −62.3, consistent with an $-SiH_3$ silicon environment, indicating significant amounts of methylsilane branches. The ^{13}C NMR and GPC-MALLS data (see below) indicate approximately 150 methylsilane branches per 1000 carbon atoms. The copolymer melting temperatures are 10−15 °C lower than those of ethylene homopolymers produced by the same catalysts (Table 4, entries 2 and 3), also suggesting significant quantities of short- and long-chain branching.

For polymerizations conducted in the presence of allylsilane, titanium nuclearity and polymer molecular weight are linearly related. However, ethylene/allylsilane polymerizations mediated by $EBICGCTi_2Me_4/2Ph_3C^+B(C_6F_5)_4^-$ require longer reaction times as compared to mononuclear organotitanium-mediated systems to produce significant amounts of polymer having useful molecular weight (M_n = 14 400; Table 3, entry 10). In contrast, $CGCTiMe_2/Ph_3C^+B(C_6F_5)_4^-$-mediated polymerizations result in copolymers of lower molecular weight (M_n = 3610; Table 3, entry 3) but with considerably higher activities (10^7 g of polymer/(mol of Ti·atm ethylene·h)) and with significantly greater comonomer incorporation. After catalyst injection into the polymerization reactor, both mono- and binuclear Ti catalyst solutions remain brightly colored throughout the course of the polymerization reactions, implying the presence of stable active catalytic species.[12c,15j] At constant catalyst and ethylene concentrations, product copolymer molecular weight is inversely proportional to silane concentration for $CGCTiMe_2$ (Table 3, entries 1−7; Figure 3a), supporting the chain-transfer mechanism depicted in Scheme 2. Intriguingly, under similar conditions, product copolymer molecular weight decreases approximately sublinearly with increasing silane concentration for $EBICGCTi_2Me_4$ (Table 3, entries 8−14; Figure 3b). These chain-transfer relationships suggest a distinctly different overall mechanistic pathway for polymerization with the bimetallic Ti catalyst, which will be elaborated on in the Discussion section.

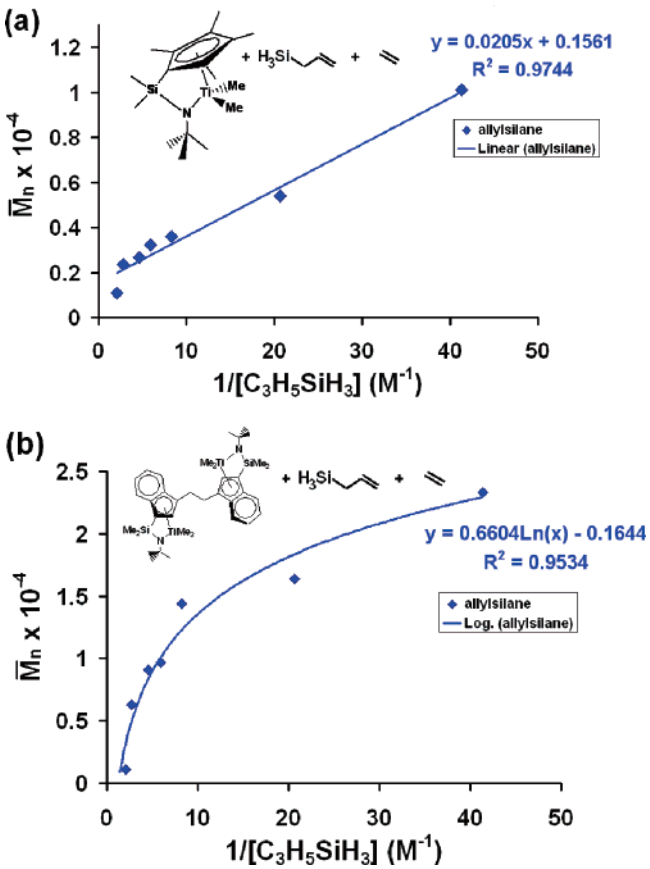

Figure 3. Relationship of ethylene + allylsilane copolymer number-average molecular weight (GPC vs polyethylene standards) to inverse allylsilane concentration at fixed ethylene and (a) $CGCTiMe_2$ and (b) $EBICGCTi_2Me_4$ concentrations.

Chain-Transfer Efficiency of 3-Butenylsilane in Organotitanium-Mediated Ethylene Copolymerizations. The comonomer 3-butenylsilane was also investigated as a chain-transfer agent for ethylene copolymerization in the presence of mono- and binuclear organotitanium catalysts (Table 5). The ^1H, ^{13}C, and ^{29}Si NMR spectra of the silane-terminated ethylene/3-butenylsilane copolymers exhibit characteristic proton ethylsilane branch (δ 0.46, 1.98, 3.59), polyethylene backbone (δ 1.2−1.4), and $-CH_3$ chain end (δ 0.98) resonances (Figure S3). The concentrations of vinyl chain end resonances are again very

Table 3. Organotitanium-Catalyzed Ethylene Polymerization in the Presence of Allylsilane

entry	precatalyst[a,b]	[precatalyst] (μM)	[$C_3H_5SiH_3$] (mM)	activity[c] ($\times 10^4$)	M_n[d]	M_w/M_n[d]	T (°C)	T_m (°C)	comonomer incorporation (%)[e]
1	$CGCTiMe_2$	200	24.2	2600	10 100	2.3	27	132	32
2	$CGCTiMe_2$	200	48.4	2700	5 400	3.2	28	130	34
3	$CGCTiMe_2$	200	121	1700	3 610	3.6	30	130	54
4	$CGCTiMe_2$	200	169	3000	3 220	4.0	30	128	52
5	$CGCTiMe_2$	200	217	3500	2 680	4.0	33	130	50
6	$CGCTiMe_2$	200	362	3300	2 350	3.6	35	131	52
7	$CGCTiMe_2$	200	484	2200	1 100	2.0	23	127	52
8	$EBICGCTi_2Me_4$	100	24.2	760	23 300	3.1	30	129	4.0
9	$EBICGCTi_2Me_4$	100	48.4	670	16 400	2.4	30	128	5.0
10	$EBICGCTi_2Me_4$	100	121	500	14 400	2.4	25	128	12
11	$EBICGCTi_2Me_4$	100	169	500	9 700	3.2	25	130	32
12	$EBICGCTi_2Me_4$	100	217	40	9 100	3.5	30	127	28
13	$EBICGCTi_2Me_4$	100	362	10	6 300	4.2	25	129	32
14	$EBICGCTi_2Me_4$	100	484	10	1 100	1.1	23	127	30

[a] CGC = $Me_2Si(Me_4C_5)(N^tBu)$, EBI = ethylene-bridged bis(indenyl). Polymerization conditions: 50 mL of toluene, 10 s for entries 1−7, 10 min for entries 8−14. [b] Cocatalyst = 10 μmol of $Ph_3CB(C_6F_5)_4$. [c] Units = g/(mol of Ti·h·atm ethylene). [d] By GPC in 1,2,4-trichlorobenzene vs polyethylene standards. [e] Comonomer incorporation calculated on the basis of ^{13}C NMR spectra.

Table 4. Organotitanium-Catalyzed Ethylene Homopolymerization

entry	precatalyst[a,b]	[precatalyst] (μM)	activity[c] ($\times 10^4$)	M_n[d]	M_w/M_n[d]	T (°C)	T_m (°C)
1	Cp^*TiMe_3	200	500	27 700	2.8	30	141
2	$CGCTiMe_2$	200	210	102 800	2.6	32	142
3	$EBICGCTi_2Me_4$	100	200	150 000	2.5	28	144

[a] CGC = $Me_2Si(Me_4C_5)(N^tBu)$, EBI = ethylene-bridged bis(indenyl). Polymerization conditions: 50 mL of toluene, 0.5 min. [b] Cocatalyst = 10 μmol of $Ph_3CB(C_6F_5)_4$. [c] Units = g/(mol of Ti·h·atm ethylene). [d] By GPC in 1,2,4-trichlorobenzene vs polyethylene standards.

Table 5. Organotitanium-Catalyzed Ethylene Polymerization in the Presence of 3-Butenylsilane

entry	precatalyst[a,b]	[precatalyst] (μM)	[$C_4H_7SiH_3$] (mM)	activity[c] ($\times 10^4$)	M_n[d]	M_w/M_n[d]	T (°C)	T_m (°C)	comonomer incorporation (%)[e]
1	$CGCTiMe_2$	200	15.8	2000	9 800	2.4	30	121	5.0
2	$CGCTiMe_2$	200	31.5	1600	3 000	3.1	32	115	12
3	$CGCTiMe_2$	200	78.9	1200	2 600	3.5	34	112	20
4	$CGCTiMe_2$	200	110	1900	2 300	4.2	32	112	20
5	$CGCTiMe_2$	200	142	1600	980	1.5	33	110	22
6	$CGCTiMe_2$	200	237	440	610	1.3	30	106	23
7	$EBICGCTi_2Me_4$	100	15.8	6.0	104 300	1.4	24	130	1.0
8	$EBICGCTi_2Me_4$	100	31.5	1.0	92 000	1.4	23	130	1.0
9	$EBICGCTi_2Me_4$	100	78.9	0.1	88 000	2.0	24	131	5.0
10	$EBICGCTi_2Me_4$	100	110	0.02	82 000	2.0	22	127	5.0
11	$EBICGCTi_2Me_4$	100	142	0.02	55 700	2.7	23	128	5.0
12	$EBICGCTi_2Me_4$	100	237	0.02	45 600	3.2	27	126	7.0

[a] CGC = $Me_2Si(Me_4C_5)(N^tBu)$, EBI = ethylene-bridged bis(indenyl). Polymerization conditions: 50 mL of toluene, 10 s for entries 1−6, 10 min for entries 7−12. [b] Cocatalyst = 10 μmol of $Ph_3CB(C_6F_5)_4$. [c] Units = g/(mol of Ti·h·atm ethylene). [d] By GPC in 1,2,4-trichlorobenzene vs polyethylene standards. [e] Comonomer incorporation calculated on the basis of ^{13}C NMR spectra.

small in the ^1H NMR spectrum, indicating that chain transfer via β-hydride elimination is insignificant and that 3-butenylsilane chain termination is the dominant chain-transfer pathway. Furthermore, the intense $-SiH_2-$ resonance in the ^1H and ^{29}Si NMR spectra suggests that 3-butenylsilane readily effects chain transfer at the polymer chain end as well as at the branch points, in addition to undergoing C═C enchainment into the polymer chain.

In addition, the resulting 3-butenylsilane-capped copolymers have narrow, monomodal polydispersities consistent with a single-site process and exhibit an intense $-SiH_2-$ ^{29}Si NMR resonance at δ −24.0, indicating that significant fractions of ethylsilane branches have likely chain-transferred to additional polymer chains. The ^{13}C NMR and GPC-MALLS data indicate approximately 50 ethylsilane branches per 1000 carbon atoms. The polymer melting temperatures are considerably lower (20−40 °C) than that of the ethylene homopolymer produced with the same catalysts (Table 4, entries 2 and 3), implying a significant degree of longer-chain branching in the copolymer products.

Interestingly, for polymerizations conducted in the presence of 3-butenylsilane, titanium nuclearity and polymer molecular weight are linearly correlated as in the case of allylsilane. Thus, ethylene/3-butenylsilane polymerizations mediated by $EBICGCTi_2Me_4/2Ph_3C^+B(C_6F_5)_4^-$ require longer reaction times compared to mononuclear organotitanium-mediated systems to produce significant amounts of polymer, but having much higher molecular weight (M_n = 82 000; Table 5, entry 10). On the other hand, $CGCTiMe_2/Ph_3C^+B(C_6F_5)_4^-$-mediated polymerizations result in copolymers with substantially lower molecular weight (M_n = 2300; Table 5, entry 4) but at considerably higher activities (10^7 g of polymer/(mol of Ti·atm ethylene·h)) and with far greater comonomer incorporation levels. After catalyst injection into the polymerization reactor, both mono- and

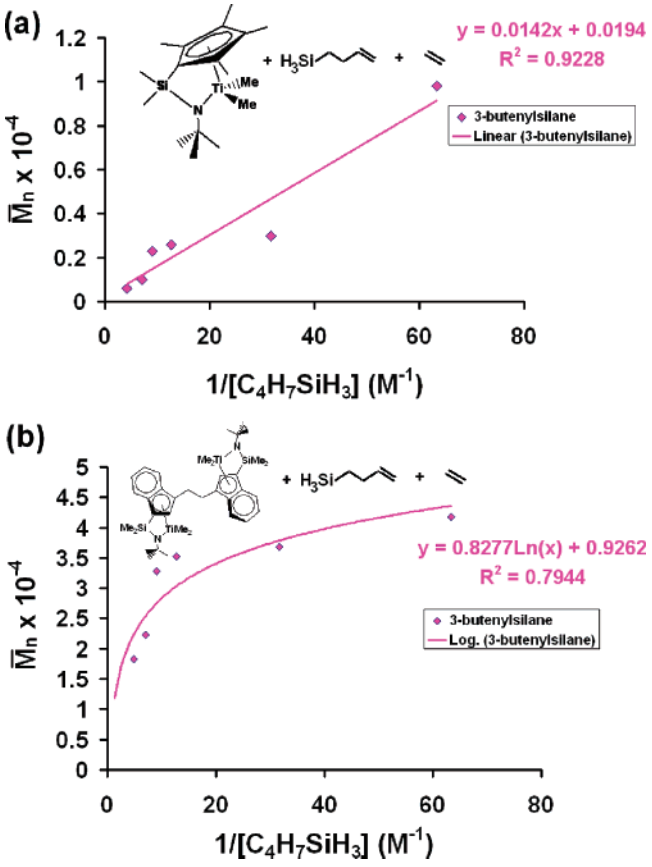

Figure 4. Relationship of ethylene + 3-butenylsilane copolymer number-average molecular weight (GPC vs polyethylene standards) to inverse 3-butenylsilane concentration at fixed ethylene and (a) $CGCTiMe_2$ and (b) $EBICGCTi_2Me_4$ concentrations.

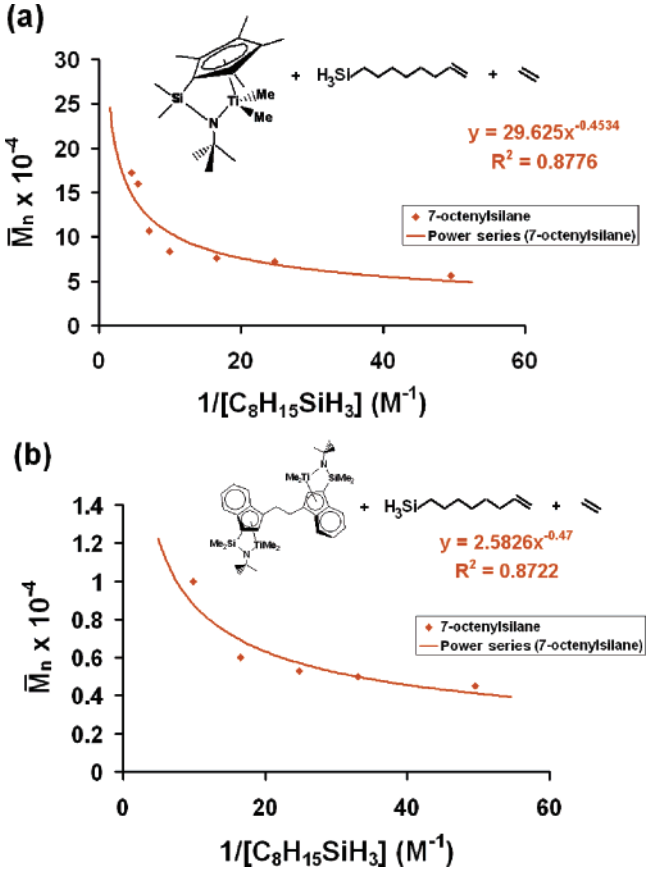

Figure 5. Relationship of ethylene + 7-octenylsilane copolymer number-average molecular weight (GPC vs polyethylene standards) to inverse 7-octenylsilane concentration at fixed ethylene and (a) $CGCTiMe_2$ and (b) $EBICGCTi_2Me_4$ concentrations.

binuclear Ti catalysts remain brightly colored throughout the course of the polymerization reactions, implying the presence of active catalytic species.[12c,15j] At constant catalyst and ethylene concentrations, product copolymer molecular weight is inversely proportional to silane concentration for $CGCTiMe_2$ (Table 5, entries 1−6; Figure 4a), supporting the chain-transfer mechanism shown in Scheme 2. Intriguingly, under similar conditions, product copolymer molecular weight decreases approximately sublinearly with increasing silane concentration for polymerizations mediated by $EBICGCTi_2Me_4$ (Table 5, entries 7−12; Figure 4b), supporting a cooperative mechanism that enhances chain-transfer efficiency at higher silane concentrations. These chain-transfer relationships suggest a significantly different mechanistic pathway for polymerization with the bimetallic Ti catalyst, which will be elaborated on in the Discussion section.

Chain-Transfer Efficiency of 7-Octenylsilane in Organotitanium-Mediated Ethylene Copolymerizations. The comonomer 7-octenylsilane was also investigated as a chain-transfer agent for ethylene polymerization using both mono- and binuclear organotitanium catalysts (Table 6). The ^{1}H NMR spectra of the silane-terminated ethylene/7-octenylsilane copolymers exhibit characteristic proton hexylsilane branch (δ 0.28, 2.15, 3.59), polyethylene backbone (δ 1.2−1.4), and $-CH_3$ chain end (δ 0.97) resonances (Figure S4). The concentrations of vinyl chain end resonances are below the detection limits in both the ^{1}H and ^{13}C NMR spectra, indicating that chain transfer via β-hydride elimination is again insignificant and that intramolecular 7-octenylsilane chain termination is the dominant chain-transfer pathway. Furthermore, the intense $-SiH_2$ and $-SiH$ resonances in the ^{1}H NMR spectrum suggest that 7-octenylsilane readily effects chain transfer at the polymer chain end as well as at the branch points, in addition to undergoing C═C enchainment into the polymer chain. The resulting 7-octenylsilane-capped copolymers have narrow, monomodal polydispersities consistent with a single-site process and prominent ^{1}H NMR resonances at δ 3.59 ($-SiH_3$), 3.95 ($-SiH_2-$), and 4.70 (>SiH-), indicating that small but significant quantities of hexylsilane branches have chain-transferred to additional polymer chains. In addition, the ^{1}H NMR and GPC-MALLS data indicate approximately 10 hexylsilane branches per 1000 carbon atoms. The copolymer melting temperatures are considerably lower (20−40 °C) than that of the ethylene homopolymer produced with the same catalysts (Table 4, entries 2 and 3), implying a significant degree of longer-chain branching in the copolymer products.

For polymerizations conducted in the presence of 7-octenylsilane, titanium nuclearity and polymer molecular weight are inversely correlated. Ethylene/7-octenylsilane polymerizations mediated by $EBICGCTi_2Me_4/2Ph_3C^+B(C_6F_5)_4^-$ require longer reaction times compared to the mononuclear organotitanium-mediated systems to produce significant amounts of polymer with lower molecular weight (M_n = 6000; Table 6, entry 11). In contrast, $CGCTiMe_2/Ph_3C^+B(C_6F_5)_4^-$-mediated polymerizations result in copolymers with higher molecular weight (M_n = 8400; Table 6, entry 4) at considerably higher activities (10^5 g of polymer/(mol of Ti·atm ethylene·h)) and with greater

Table 6. Organotitanium-Catalyzed Ethylene Polymerization in the Presence of 7-Octenylsilane

entry	precatalyst[a,b]	[precatalyst] (μM)	[$C_8H_{15}SiH_3$] (mM)	activity[c] ($\times 10^4$)	M_n[d]	M_w/M_n[d]	T (°C)	T_m (°C)	comonomer incorporation (%)[e]
1	$CGCTiMe_2$	200	20.2	290	5 600	2.9	30	120	0.5
2	$CGCTiMe_2$	200	40.4	10	7 200	2.5	25	116	1.0
3	$CGCTiMe_2$	200	60.6	35	7 600	2.1	25	122	3.0
4	$CGCTiMe_2$	200	101	0.2	8 400	2.5	28	122	4.0
5	$CGCTiMe_2$	200	141	0.3	10 700	2.6	24	126	4.0
6	$CGCTiMe_2$	200	182	0.2	16 000	3.5	24	124	5.0
7	$CGCTiMe_2$	200	220	0.2	17 200	2.2	24	123	5.0
8	$EBICGCTi_2Me_4$	100	20.2	2.0	4 500	2.0	24	106	0.5
9	$EBICGCTi_2Me_4$	100	40.4	0.1	5 000	2.4	24	110	1.0
10	$EBICGCTi_2Me_4$	100	60.6	0.2	5 300	2.5	26	107	1.0
11	$EBICGCTi_2Me_4$	100	101	0.1	6 000	2.4	25	100	2.0
12	$EBICGCTi_2Me_4$	100	141	0.4	10 000	2.1	25	101	2.0

[a] CGC = $Me_2Si(Me_4C_5)(N^tBu)$, EBI = ethylene-bridged bis(indenyl). Polymerization conditions: 50 mL of toluene, 10 min for entries 1−7, 60 min for entries 8−12. [b] Cocatalyst = 10 μmol of $Ph_3CB(C_6F_5)_4$. [c] Units = g/(mol of Ti·h·atm ethylene). [d] By GPC in 1,2,4-trichlorobenzene vs polyethylene standards. [e] Comonomer incorporation calculated on the basis of ^{13}C NMR spectra.

Table 7. GPC-MALLS-Derived Branching Data for Organotitanium-Catalyzed Copolymerizations

entry	precatalyst[a,b]	alkenylsilane	[alkenylsilane] (mM)	B per 1000 C[c]	LCB per 1000 C[c]	% LCB per B[c]	$\langle r_g^2\rangle$[c] (nm)	g_M[c]
1	$CGCTiMe_2$	allylsilane	121	150 (35)	10 (5)	6.0 (3.0)	78.5 (8.6)	0.1
2	$EBICGCTi_2Me_4$	allylsilane	121	100 (13)	10 (3)	10 (2)	38.0 (11)	0.1
3	$CGCTiMe_2$	3-butenylsilane	110	50 (7)	10 (2)	20 (3)	15.5 (2.3)	0.5
4	$EBICGCTi_2Me_4$	3-butenylsilane	110	20 (7)	5.0 (1.5)	25 (6)	91.9 (23)	0.3
5	$CGCTiMe_2$	5-hexenylsilane	51.1	40 (5)	10 (3)	25 (4)	91.7 (18)	0.2
6	$EBICGCTi_2Me_4$	5-hexenylsilane	51.1	20 (7)	5.0 (2.3)	25 (7)	115 (13)	0.2
7	$CGCTiMe_2$	7-octenylsilane	101	10 (3)	2.0 (0.3)	20 (3)	88.7 (18)	1.0
8	$EBICGCTi_2Me_4$	7-octenylsilane	101	10 (3)	2.0 (0.7)	20 (5)	80.7 (24)	1.0

[a] CGC = $Me_2Si(Me_4C_5)(N^tBu)$, EBI = ethylene-bridged bis(indenyl). [$CGCTiMe_2$] = 200 μM, [$EBICGCTi_2Me_4$] = 100 μM. [b] Cocatalyst = 10 μmol of $Ph_3C^+B(C_6F_5)_4^-$. [c] B = total branches, C = carbon atoms, LCB = long-chain branches, $\langle r_g^2\rangle$ = root-mean-square radius of gyration, g_M = branching ratio. All values were determined by GPC-MALLS. Calculations follow ref 24. Standard deviations are reported in parentheses.

comonomer enchainment selectivities. After catalyst injection into the polymerization reactor, both mono- and binuclear Ti catalysts remain brightly colored throughout the course of the polymerization reactions, implying the presence of stable active catalytic species.[12c,15j] At constant catalyst and ethylene concentrations, product copolymer molecular weight increases as an approximate superlinear series with increasing silane concentration for $CGCTiMe_2$ (Table 6, entries 1−7; Figure 5a), suggesting more long-chain branching at higher silane concentrations, which increases the polymer molecular weight. Intriguingly, under similar conditions, product copolymer molecular weight also increases as an approximate superlinear series with increasing silane concentration for polymerizations mediated by $EBICGCTi_2Me_4$ (Table 6, entries 8−12; Figure 5b). The chain-transfer plots, in addition to the ^1H NMR resonances at δ 3.95 and δ 4.70, indicate the presence of significant quantities of hexylsilane branches which have chain-transferred additional polymer chains. These plots again suggest a different overall mechanistic pathway for polymerization/chain transfer mediated by the bimetallic Ti catalyst as well as for longer alkenylsilanes, which will be analyzed in the Discussion section.

Summary of the Scope of Alkenylsilane Chain Transfer and Comonomer Effects in Organotitanium-Mediated Ethylene Polymerization. Organotitanium complexes mediate the copolymerization of alkenylsilanes and ethylene with high activity. However, the product polymer microstructures as well as the chain-transfer behavior of the various alkenylsilanes are highly dependent on both the alkenylsilane chain length and Ti catalyst nuclearity. In all of these polymerization systems, polymer molecular weights differ significantly from those in the corresponding ethylene homopolymerizations, ethylene/1-hexene copolymerizations, and ethylene homopolymerization in the presence of *n*-hexylsilane carried out with the same organotitanium catalysts. For all alkenylsilane + ethylene copolymers produced, alkenylsilane chain termination is the dominant chain-transfer pathway, as indicated by ^1H, ^{13}C, and ^{29}Si NMR spectroscopy and chain-transfer plots (Figures 1−5).

Mechanistic Considerations. As a prelude to a detailed discussion of alkenylsilane + ethylene copolymerization mechanism and kinetics, it is useful to briefly summarize the relevant observations.

(i) Mononuclear activated $CGCTiMe_2$ mediates ideally behaved silanolytic chain transfer, indicated by the linear relationship between M_n and [alkenylsilane]$^{-1}$ for C_3 to C_6 alkenylsilanes.

(ii) Binuclear activated $EBICGCTi_2Me_4$ mediates less than ideally behaved silanolytic chain transfer, indicated by the sublinear relationship between M_n and [alkenylsilane]$^{-1}$ for C_3 and C_4 alkenylsilanes.

(iii) Binuclear activated $EBICGCTi_2Me_4$ mediates less than ideal silanolytic chain transfer, indicated by the superlinear relationship between M_n and [alkenylsilane]$^{-1}$ for C_6 and C_8 alkenylsilanes.

(iv) All organotitanium systems efficiently produce silane-capped polyolefins.

(v) Binuclear $EBICGCTi_2Me_4$ generally produces higher molecular weight polymer versus mononuclear $CGCTiMe_2$ for all of the alkenylsilanes.

(vi) Mononuclear $CGCTiMe_2$ consistently incorporates higher levels of comonomer versus binuclear $EBICGCTi_2Me_4$ for all of the alkenylsilanes.

(vii) As alkenylsilane chain length increases, the level of comonomer incorporation parallels that of the analogous α-olefin + ethylene copolymerizations.[21]

(viii) As C_3 and C_4 [alkenylsilane] increases, polyolefin molecular weight decreases for all organotitanium-mediated systems.

(ix) As [5-hexenylsilane] increases, polyolefin molecular weight decreases for $CGCTiMe_2$-mediated systems and increases for $EBICGCTi_2Me_4$-mediated systems.

(x) As [7-octenylsilane] increases, polyolefin molecular weight increases for all organotitanium-mediated systems.

Discussion

Effects of Alkenylsilane Chain Dimensions on Comonomer Incorporation and Branch Formation. The present results indicate that the extent of alkenylsilane incorporation and branch formation during organotitanium-mediated copolymerization with ethylene increases in the order

$$C_8H_{15}SiH_3 < C_6H_{11}SiH_3 \approx C_4H_7SiH_3 < C_3H_5SiH_3$$

This is consistent with general literature precedent for unfunctionalized α-olefin relative insertion rates.[21] The ^{13}C NMR and GPC-MALLS-derived comonomer incorporation data are in good agreement. The GPC-MALLS-derived long-chain branching (LCB) data indicate that the ratio of LCB to total branch content increases in the order

$$C_3H_5SiH_3 < C_4H_7SiH_3 \approx C_6H_{11}SiH_3 \approx C_8H_{15}SiH_3$$

The smallest alkenylsilane, allylsilane, exhibits the greatest coenchainment selectivity, resulting in approximately 150 total branches + 10 LCB and 100 total branches + 10 LCB per 1000 carbon atoms for mono- and binuclear catalyst systems, respectively (Table 7, entries 1 and 2). The relatively high T_m of the allysilane/ethylene copolymers is likely due to significant blocks of enchained allylsilane as well as some amount of cross-linking due to the high $-SiH_x$ concentrations. In comparison, 3-butenylsilane results in polyethylenes with approximately 50 total branches + 10 LCB and 20 total branches + 5 LCB per 1000 carbon atoms for mono- and binuclear systems, respectively (Table 7, entries 3 and 4). The mid-length 5-hexenylsilane results in polyethylenes with approximately 40 total branches + 10 LCB and 20 total branches + 5.0 LCB per 1000 carbon atoms for mono- and binuclear systems, respectively (Table 7, entries 5−6). The longest alkenylsilane, 7-octenylsilane, produces polyethylenes with approximately 10 total branches + 2.0 LCB per 1000 carbon atoms for both mono- and binuclear systems, respectively (Table 7, entries 7−8). As the alkenylsilane chain length increases, the selectivity for comonomer incorporation falls, reasonably a consequence of differential nonbonded repulsions. It is likely that the smaller alkenylsilanes undergo more facile coordination/insertion[22,23] in the catalyst coordination sphere due to attenuated steric repulsion from the ancillary ligands, the polymeryl fragment, and the counteranion (e.g., **5**). It is likewise reasonable that longer-chain alkenylsilanes undergo more sluggish coordination/enchainment due to greater steric impediments (e.g., **6**).

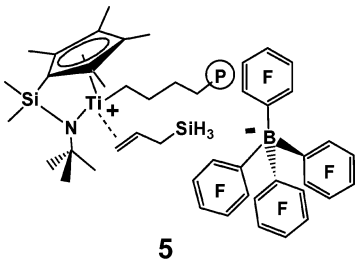

5

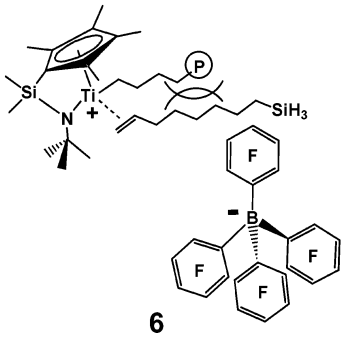

6

The selectivity for the types of polyolefin branches created during organotitanium-mediated copolymerization of alkenylsilanes with ethylene is highly dependent on alkenylsilane chain dimensions, as assessed by ^1H, ^{13}C, and ^{29}Si NMR spectroscopy and by GPC-MALLS. In the allylsilane + ethylene system, significant densities of short methylsilane branches dominate the copolymer microstructural branching (Figure S2). Such branches appear to be too short to chain-transfer intermolecularly to other growing polymer chains with very high selectivity (e.g., **7**) to achieve chain coupling, although GPC-MALLS data indicate this is not entirely impossible but simply less efficient compared to chain coupling by longer alkylsilane branches (see below). The two propagating polymer chains must achieve close proximity for a methylsilane branch to achieve efficient intermolecular chain transfer to a second propagating polymer chain. These short branches also appear to be too short to effect efficient intramolecular chain transfer due to the enhanced ring strain associated with this type of "back-biting" (e.g., **8**). The 3-butenylsilane + ethylene and 5-hexenylsilane + ethylene systems produce copolymers with appreciable densities of ethylsilane and *n*-butylsilane branches, respectively. In addition, these branches are sufficiently long to support extensive intermolecular chain transfer from silyl groups on the branches. Note that there are prominent signals for secondary silane ($-SiH_2-$) groups in the ^1H, ^{13}C, and ^{29}Si NMR spectra (Figures S1 and S3). In the 7-octenylsilane + ethylene copolymerization system, the long *n*-hexylsilane branches are the shortest branches detected in the polymer microstructure. These *n*-hexylsilane

(21) (a) Dahlmann, M.; Erker, G.; Bergander, K. *J. Am. Chem. Soc.* **2000**, *122*, 7986. (b) Karl, J.; Dahlmann, M.; Erker, G.; Bergander, K. *J. Am. Chem. Soc.* **1998**, *120*, 5643. (c) Kissin, Y. V. *Isospecific Polymerization of Olefins*; Springer-Verlag: New York, 1985; pp 1−93.

(22) For theoretical studies, see: (a) Tobisch, S.; Ziegler, T. *J. Am. Chem. Soc.* **2004**, *126*, 9059. (b) Lanza, G.; Fragala, I. L. *Top. Catal.* **1999**, *7*, 45. (c) Froese, R. D. J.; Musaev, D. G.; Morokuma, K. *Organometallics* **1999**, *18*, 373. (d) Kawamura-Kuribayashi, H.; Koga, N.; Morokuma, K. *J. Am. Chem. Soc.* **1992**, *114*, 2359.

(23) Coordination and insertion studies: (a) Landis, C. R.; Rosaaen, K. A.; Sillars, D. R. *J. Am. Chem. Soc.* **2003**, *125*, 1710. (b) Schaper, F.; Geyer, A.; Brintzinger, H. H. *Organometallics* **2002**, *21*, 473. (c) Bochmann, M. *J. Chem. Soc., Dalton Trans.* **1996**, 255.

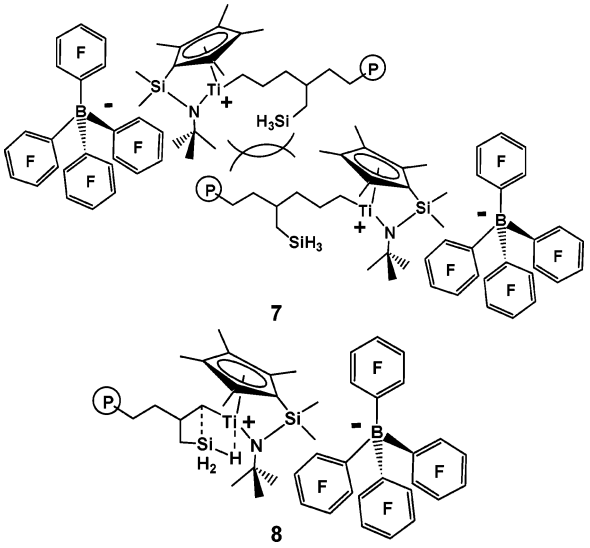

7

8

branches are again sufficiently long to undergo intermolecular chain transfer to a second growing chain with greater efficiencies than methylsilane branches (eq 4; Scheme 2). Although alkyl-

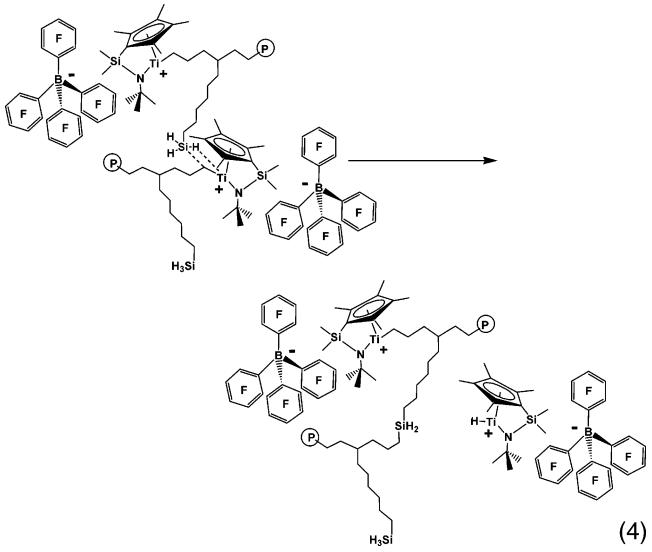

(4)

silane-branch chain transfer is expected to be considerably less efficient than alkenylsilane-mediated chain transfer, as seen from the aforementioned control experiments with *n*-hexylsilane (Figure 2), small but significant amounts of long-chain branching produced by alkylsilane-branch chain transfer should significantly increase the copolymer molecular weight. In addition, this type of chain transfer may be facilitated for alkenylsilanes of appropriate dimensions by the binuclear Ti catalyst holding two polymer chains in close proximity, although this effect is generally small. Thus, this mode of cooperativity may be operative for the binuclear catalyst-mediated allylsilane + ethylene and possibly the 3-butenylsilane + ethylene systems (Table 7, entries 2 and 4). The ^{1}H NMR spectrum of the 7-octenylsilane + ethylene copolymer reveals intense resonances for $-$SiH, $-$SiH$_2$, and $-$SiH$_3$ moieties, suggesting formation of a variety of pendant groups including long- and short-chain branches (Figure S4).

In the aforementioned copolymerization systems, longer branch lengths generally correlate with greater extents of long-

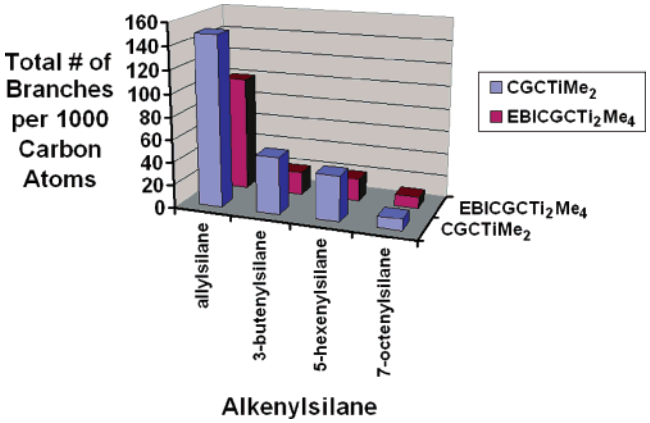

Figure 6. Relationship of the density of short-chain branches to alkenylsilane chain length for CGCTiMe$_2$- and EBICGCTi$_2$Me$_4$-mediated copolymerization of alkenylsilanes with ethylene.

chain branching, reflecting the potential kinetic advantage of longer branches to more easily contact a second metal$-$polymeryl center with minimal steric impediment (e.g., eq 4). Considering the total branch density formed during *mononuclear* catalyst-mediated polymerization, 6% of all branches are LCB in allylsilane + ethylene copolymers, 20% of all branches are LCB in 3-butenylsilane + ethylene copolymers, 25% of all branches are LCB in 5-hexenylsilane + ethylene copolymers, and 20% of all branches are LCB in 7-octenylsilane + ethylene copolymers. Considering the total branch density formed during *binuclear* catalyst-mediated polymerization, 10% of all branches are LCB in allylsilane + ethylene copolymers, 25% of all branches are LCB in 3-butenylsilane and 5-hexenylsilane + ethylene copolymers, and 20% of all branches are LCB in 7-octenylsilane + ethylene copolymers. These LCB densities reflect the relative efficiency of alkylsilane branches to undergo intermolecular chain transfer. Furthermore, the shorter the alkenylsilane chain length, the greater the density of short-chain branching due to more facile activation/enchainment in both the mono- and binuclear catalyst systems (Figure 6).

The LCB trends are reflected in the dramatic differences in physical properties of the copolymers mentioned above. As the chain density of LCB increases, the polymer melting temperatures dramatically decrease compared to polyethylene (Tables 1$-$6). These trends illustrate the capacity to control the LCB density and tune polyolefin microstructure simply by altering the alkenylsilane chain length. MALLS-derived branching ratios, g_M, are found to increase with increasing alkenylsilane chain length and follow the trend

$$0.1 \approx g_M(C_3) < g_M(C_4) \approx g_M(C_6) < g_M(C_8) \approx 1.0$$

The branching ratio is defined by eq 5,[24] where $\langle r_g^2\rangle_{branch}$ is the root-mean-square radius of gyration of the branched polymer and $\langle r_g^2\rangle_{linear}$ is the root-mean-square radius of gyration of the

(24) (a) Striegel, A. M., Ed. *Multiple Detection in Size-Exclusion Chromatography*; ACS Symposium Series 893; American Chemical Society: Oxford University Press, 2005; pp 3$-$75. (b) Wu, C.-S., Ed. *Handbook of Size Exclusion Chromatogrphy and Related Techniques*; Marcel Dekker, Inc.: New York, 2004; Chapter 4, p 21. (c) Provder, T., Ed. *Chromatography of Polymers: Hyphenated and Multidimensional Techniques*; ACS Symposium Series 731; American Chemical Society: Oxford University Press, 1999; Chapters 17 and 18. (d) Provder, T., Ed. *Detection and Data Analysis in Size Exclusion Chromatography*; ACS Symposium Series 352; American Chemical Society: Oxford University Press, 1999; Chapter 8. (e) Belenkii, B. G.; Vilenchik, L. Z. *Modern Liquid Chromatography of Macromolecules*; Elsevier: New York, 1983; pp 291$-$323.

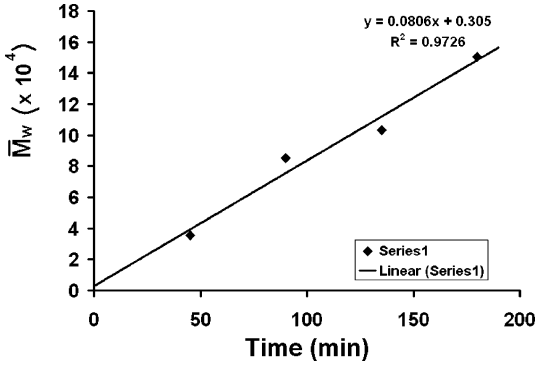

Figure 7. Relationship of the copolymer molecular weight to polymerization time for $CGCTiMe_2$-mediated copolymerization of 7-octenylsilane with ethylene.

corresponding linear polymer of equivalent molecular weight (Table 7). Thus, g_M compares the root-mean-square radii of

$$g_M = \left(\frac{\langle r_g^2 \rangle_{branch}}{\langle r_g^2 \rangle_{linear}} \right)_M \qquad (5)$$

branched and linear macromolecules of identical molecular weight, and since branched molecules are more compact than the linear analogues, g_M values can provide relative branch density based on how close the value approaches 0.0 or 1.0. This branching ratio data trend is additional evidence for the presence of greater densities of total branches as the alkenylsilane chain length decreases. The branching ratios also indicate that all of the C_3-C_6 alkenylsilane + ethylene copolymers have significantly smaller radii than the linear analogues, arguing for significant branch formation in all of these copolymerization systems. Furthermore, the significantly smaller total branch density for 7-octenylsilane gives rise to a branching ratio of approximately 1.0, which is attributable to more sluggish coordination/enchainment due to greater steric impediments.

As shown by the GPC-MALLS data for the present copolymerization systems, longer branch lengths generally correlate with larger extents of long-chain branching, reflecting the potential kinetic advantage of longer branches to more easily contact a second metal−polymeryl center with minimal steric impediment (e.g., eq 4). For the mononuclear catalyst-mediated 7-octenylsilane + ethylene system, the copolymer molecular weight scales linearly with polymerization time (Figure 7). Figure 7 indicates that, as the polymerization reaction proceeds with increasing time, the likelihood of a hexylsilane branch to contact another Ti−polymeryl species and effect chain transfer also increases. It is likely that the large increase in copolymer molecular weight is attributable to long-chain branch formation via hexylsilane-branch chain transfer.

Alkenylsilane Chain Length Effects on Chain-Transfer Efficiency. In the present organotitanium-mediated alkenylsilane + ethylene copolymerization systems, where a homologous series of alkenylsilanes is employed as chain-transfer agents, all alkenylsilanes are found to efficiently effect chain termination. Comparing copolymer M_n data with alkenylsilane chain length (at identical alkenylsilane concentrations) for both mononuclear and binuclear Ti catalyst systems, copolymer molecular weights are invariably smaller than those of the corresponding ethylene homopolymers produced with the same catalysts (Figure 8, Table 4). Furthermore, the $EBICGCTi_2Me_4$-

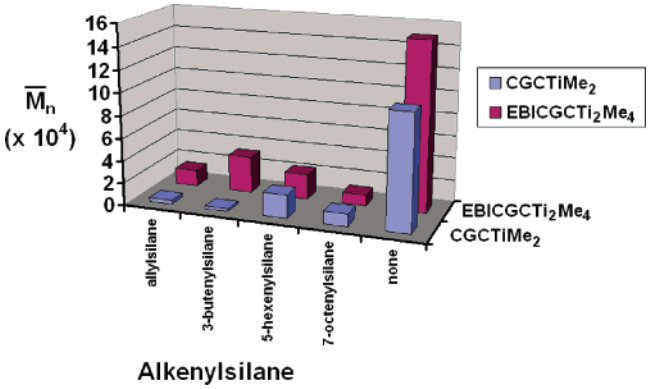

Figure 8. Dependence of copolymer number-average molecular weight on alkenylsilane chain length at constant 100 mM [alkenylsilane] for $CGCTiMe_2$- and $EBICGCTi_2Me_4$-mediated copolymerization of alkenylsilanes with ethylene.

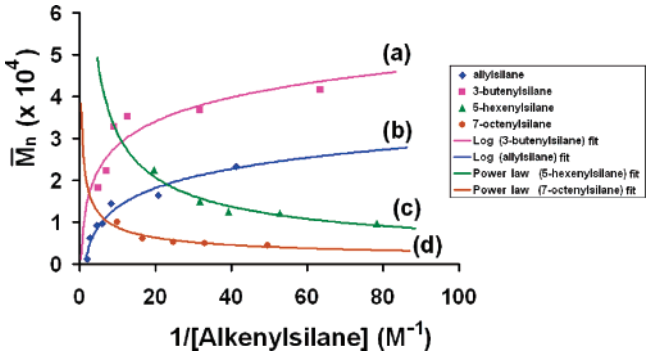

Figure 9. Comparison of ethylene + alkenylsilane copolymer number-average molecular weight (GPC vs polyethylene) relationship to inverse concentrations of (a) 3-butenylsilane, (b) allylsilane, (c) 5-hexenylsilane, and (d) 7-octenylsilane at identical fixed $EBICGCTi_2Me_4$ and ethylene concentrations.

mediated polymerization systems consistently produce higher molecular weight polymers than those of the mononuclear catalyst system (albeit with somewhat lower activity and lower comonomer incorporation selectivity). The presence of two Ti centers in close proximity most likely facilitates insertion of a chain-transferred copolymer product (Scheme 3, step iv) and/or chain transfer of a growing polymer chain by an alkylsilane branch on another growing polymer chain (Scheme 3, step ii). The binuclear Ti system chain-transfer plots (Figure 9c,d) reveal significant deviations for longer alkenylsilanes, and for shorter alkenylsilanes they exhibit slight deviations (Figure 9a,b) from the ideal, linear chain-transfer plots produced with the mononuclear Ti system (e.g., Figures 1a, 2a, 3a, and 4a), suggesting some degree of cooperativity between the two active Ti centers in effecting enchainment and chain transfer, depending on the alkenylsilane chain length. A likely explanation for this nonlinear behavior is enhanced interchain and intrachain Si−C coupling processes due to the close proximity of the two Ti centers.

Ti Nuclearity Effects on Alkenylsilane Chain Transfer. As noted above, binuclear Ti catalyst $EBICGCTi_2Me_4$ consistently produces higher molecular weight polyolefins than does the mononuclear $CGCTiMe_2$ analogue. A plausible explanation invokes a cooperative enchainment/chain-transfer process involving the two proximate active centers, resulting in more probable macromonomer reinsertion or alkylsilane-branch chain transfer to a growing chain (Scheme 3, steps iv and ii,

Scheme 3. Proposed Catalytic Cycle for Binuclear Organotitanium-Mediated Alkenylsilane + Ethylene Copolymerization[a]

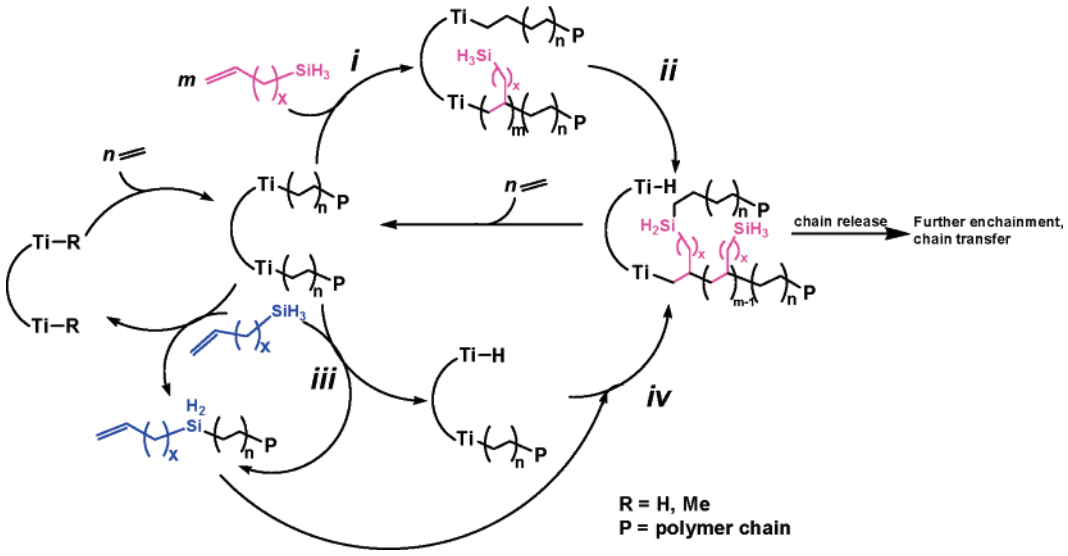

[a] (*i*) Olefin enchainment in Ti−C bond, (*ii*) σ-bond metathesis, (*iii*) σ-bond metathesis, (*iv*) olefin enchainment in Ti−C bond (Ti−H also possible but not shown).

respectively). In regard to enchainment selectivity, this type of olefin insertion cooperativity between two proximate Ti centers has been previously shown to afford high molecular weight polyolefins with dramatically enhanced α-olefin comonomer incorporation versus the mononuclear analogue.[12] It was proposed previously that the dicationic bimetallic framework likely displays enhanced α-olefin binding affinity/kinetic detainment (e.g., **3**), leading to increased comonomer enchainment.[12] Bimetallic cooperative effects resulting in such reaction sequences (Scheme 3) here would produce higher molecular weight polyolefin products with long-chain branching as a consequence of the longer comonomer-derived $-SiH_3$-terminated branches in the polymer microstructure. Note that this intradimer silanolytic chain-transfer process as a means to introduce long-chain branching is unprecedented. Interestingly, the present binuclear Ti catalyst mediates alkenylsilane chain transfer in dramatically different ways, depending on the alkenylsilane chain length. For short alkenylsilanes (C_3 and C_4) with the bimetallic catalyst, the chain-transfer plots reveal an approximate logarithmic relationship in which polymer molecular weight falls sublinearly with increasing alkenylsilane concentration (Figures 3b and 4b, respectively). A plausible explanation is that, at low alkenylsilane concentrations, the lower levels of comonomer enchainment sufficiently depress the effective local silane concentration and thus the chain-transfer rate, as to produce polymers of only modestly varying molecular weights.[25] In addition, at high alkenylsilane concentrations, greater comonomer enchainment increases the effective local silane concentration nonlinearly to enhance intrabimetallic or monometallic chain transfer (Scheme 4, pathway I, eqs (a) and (b), respectively). These types of interactions[26] between Ti centers and the weakly basic, enchained $-SiH_3$ groups may also block olefin activation, thus depressing propagation rates and causing polymer molecular weight to fall sublinearly with increasing alkenylsilane concentration via Scheme 4, pathway I.

Scheme 4. Chain-Transfer Pathways for (I) Mononuclear Ti-Mediated Silane Chain Transfer and (II) Binuclear-Mediated Silane Chain Transfer

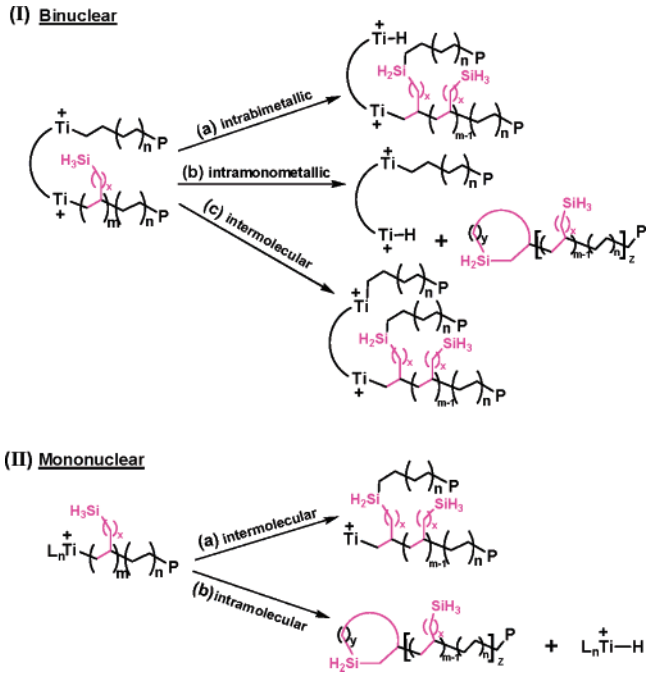

In contrast to the shorter alkenylsilanes, chain-transfer plots involving longer alkenylsilanes (C_6 and C_8) exhibit a power series relationship in which polymer molecular weight increases superlinearly with increasing alkenylsilane concentration (Figures 1b and 5b, respectively). This superlinear relationship correlates with an increase in the proportion of long-chain

(25) Tait, P. J. T.; Watkins, N. D. *Comprehensive Polymer Science*; Allen, G., Bevington, J. C., Eds.; Pergamon Press: Oxford, 1989; Vol. 4, pp 123−191 and 549−563.

(26) Metal-η^2-H-SiR_3 coordination: (a) Dubberley, S. R.; Ignatov, S. K.; Rees, N. H.; Razuvaev, A. G.; Mountford, P.; Nikonov, G. I. *J. Am. Chem. Soc.* **2003**, *125*, 642. (b) Lin, Z. *Chem. Soc. Rev.* **2002**, *31*, 239. (c) Nikonov, G. I. *Angew. Chem., Int. Ed.* **2001**, *40*, 3353. (d) Kubas, G. J. *J. Organomet. Chem.* **2001**, *635*, 37. (e) Corey, J. Y.; Braddock-Wilking, J. *Chem. Rev.* **1999**, *99*, 175. (f) Luo, X.-L.; Kubas, G. J.; Burns, C. J.; Bryan, J. C.; Unkefer, C. J. *J. Am. Chem. Soc.* **1995**, *117*, 1159. (g) Crabtree, R. H. *Angew. Chem., Int. Ed.* **1993**, *32*, 789. (h) Koga, N.; Morokuma, K. *J. Am. Chem. Soc.* **1993**, *115*, 6883. (i) Schubert, U. *Adv. Organomet. Chem.* **1990**, *30*, 151. (j) Kubas, G. J. *Acc. Chem. Res.* **1988**, *21*, 120.

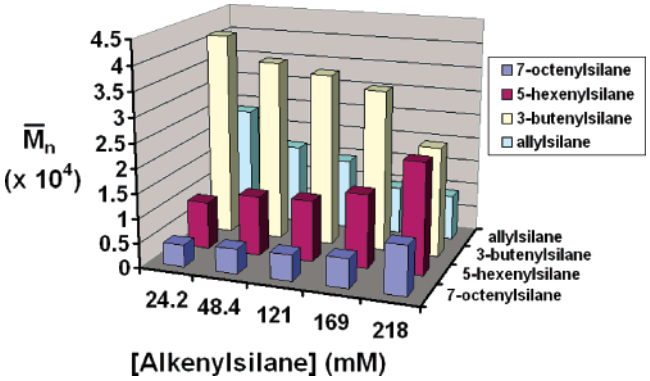

Figure 10. Dependence of copolymer number-average molecular weight on alkenylsilane chain length and concentration for EBICGCTi$_2$Me$_4$-mediated copolymerization of alkenylsilanes with ethylene.

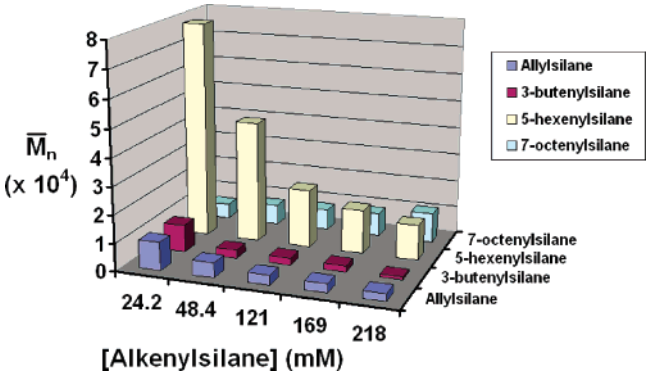

Figure 11. Dependence of copolymer number-average molecular weight on alkenylsilane chain length and concentration for CGCTiMe$_2$-mediated copolymerization of alkenylsilane with ethylene.

branches produced in the corresponding copolymer microstructures (Table 7). Interestingly, only in the case of 7-octenylsilane does the mononuclear Ti system also exhibit a superlinear power series chain-transfer relationship. A plausible explanation for these observations is that the longer ω-SiH$_3$ branches, formed by enchainment of these C$_6$ and C$_8$ alkenylsilanes, can readily chain-transfer to growing polymer chains in an intradimer/cooperative manner (Scheme 4, pathway I, eq (a)) or, for the mononuclear catalyst, via an intermolecular process (Scheme 4, pathway II, eq (a)). The longer branches maximize the probability that chain transfer can occur between two polymer chains and thus enhance the selectivity for alkylsilane-branch chain transfer (Scheme 4, pathway I, eqs (a)−(c); eq 4). This chain-transfer process is supported by the 1:1:2 ^{1}H NMR integration seen for −Si*H*$_3$:>Si*H*$_2$:>Si*H*− groups in Figure S4. Such cooperativity effects, combined with longer branches, would result in superlinearly increased polymer molecular weight with increasing alkenylsilane concentrations. In addition, even without this type of cooperativity, the longer ω-SiH$_3$ branches would also have the capability of effecting intramolecular silanolytic chain transfer to produce cyclized chain ends (Scheme 4, pathway I, eq (b)). At low alkenylsilane concentrations, less comonomer is incorporated, thus minimizing the local effective density of alkylsilane branches available to undergo intradimer chain transfer, thereby producing lower molecular weight polymer. This binuclear cooperativity, in combination with alkenylsilane chain length effects, accounts for the opposite chain-transfer trends observed for short versus long alkenylsilanes (Figures 9 and 10).

The mononuclear CGCTiMe$_2$-catalyzed copolymerization systems exhibit ideal chain-transfer behavior for alkenylsilanes ranging from C$_3$ to C$_6$ (Figures 11and 12). In these systems, polymer molecular weight decreases linearly with increasing alkenylsilane concentration. In contrast, with increasing *n*-hexylsilane concentration, the number-average molecular weight of the polyethylene product does not decrease linearly, indicating that the olefinic moiety is essential for efficiency in the alkenylsilane chain-transfer process. The data in Figure 12 indicate that 3-butenylsilane has the greatest chain-transfer efficiency, likely due to its moderate size. Allylsilane is sufficiently small to be sterically competitive with ethylene insertion, and thus allylsilane propagation is more rapid than silane chain transfer. In addition, Figure 12 shows that 5-hexenylsilane is sufficiently encumbered to exhibit depressed insertion rates vs chain-transfer rates in comparison with the

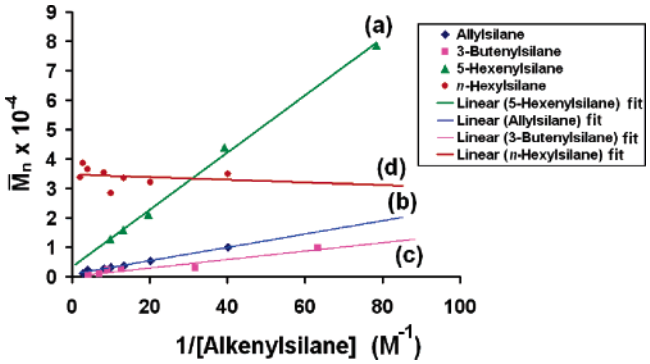

Figure 12. Comparison of ethylene + alkenylsilane copolymer number-average molecular weight (GPC vs polyethylene) relationship to inverse concentrations of (a) 5-hexenylsilane, (b) allylsilane, (c) 3-butenylsilane, and (d) *n*-hexylsilane at identical fixed CGCTiMe$_2$ and ethylene concentrations.

smaller alkenylsilanes. Alkenylsilanes ranging from C$_3$ to C$_6$ exhibit very efficient, ideal chain-transfer pathways, in support of the predominance of Scheme 2. In marked contrast, longer 7-octenylsilane deviates significantly from this ideal behavior (Figure 5a). The chain-transfer behavior in the mononuclear CGCTiMe$_2$-mediated system for 7-octenylsilane/ethylene copolymerization is similar to that in the aforementioned binuclear systems, with polymer molecular weights scaling as a power series with increasing alkenysilane concentration (Figure 5). This comonomer creates long hexylsilane branches when enchained, likely resulting in higher molecular weight polymers at high silane concentrations due to intermolecular alkylsilane-branch chain transfer to other growing polymer chains (eq 4). At lower 7-octenylsilane concentrations, the aforementioned chain transfer is less probable due to lower levels of comonomer enchainment, thus resulting in lower molecular weight copolymer. At relatively short alkenylsilane chain lengths (C$_3$−C$_6$), alkenylsilane chain-transfer behavior is nearly ideal, as seen in Figure 12, whereas at longer chain lengths (C$_8$), alkenylsilane chain-transfer behavior is still efficient but deviates from ideality (Figure 5a), suggesting that LCB content in the polymer microstructure can be tuned by varying catalyst nuclearity as well as alkenysilane chain length.

Kinetics and Mechanism of Organotitanium-Mediated Alkenylsilane + Ethylene Copolymerizations. A series of polymerizations with varying alkenylsilane concentrations (in pseudo-zero-order excess) was conducted using activated CGCTiMe$_2$ as the catalyst and with constant catalyst and ethylene

Table 8. Kinetic Rate Constant Ratios for $CGCTiMe_2$-Catalyzed Copolymerization

entry	ratio[a]	allyl-silane	3-butenyl-silane	5-hexenyl-silane
1	$k_p^{alkenylsilane}/k_{Si}^{total}$	20	1	5
2	$k_p^{ethylene}/k_{Si}^{total}$	40	30	180

[a] Rate constant ratios were calculated from M_n vs 1/[alkenylsilane] plots using the following equation: $\bar{P}_n = (k_p^{ethylene}[ethylene] + k_p^{alkenylsilane}[alkenylsilane])/(k_{Si}^{inter}[alkenylsilane] + k_{Si}^{intra}[alkenylsilane])$ (eq 7).

concentrations. As noted above, a linear relationship between M_n and 1/[alkenylsilane] is observed (Figure 12) for alkenylsilanes ranging from C_3 to C_6, consistent with alkenylsilane acting as the dominant chain-transfer agent in an intermolecular process. As noted above, the absence of vinyl resonances and the presence of $-SiH_2$ resonances in the ^1H and ^{13}C NMR spectra also implicate silanolysis as the dominant chain termination pathway.

Under steady-state conditions, the number-average degree of polymerization, P_n, is equal to the sum of all rates of propagation, $\sum R_p$, divided by the sum of the rates of all competing chain-transfer pathways, $\sum R_t$ (eq 6).[21] Assuming a single dominant chain-transfer process by alkenylsilane and rapid chain reinitiation after chain transfer, P_n is given by eq 7, where k_p is the rate constant for propagation and k_{Si} the rate constant for inter-/intramolecular silanolytic chain transfer.

$$\bar{P}_n = \frac{\sum R_p}{\sum R_t} \tag{6}$$

$$\bar{P}_n = \frac{k_p^{ethylene}[ethylene] + k_p^{alkenylsilane}[alkenylsilane]}{k_{Si}^{inter}[alkenylsilane] + k_{Si}^{intra}[alkenylsilane]} \tag{7}$$

With polymerizations carried out at constant catalyst and monomer concentration and with a pseudo-zero-order excess of alkenylsilane, Figure 12 shows that eq 7[4a] is obeyed over a broad silane concentration range (except for 7-octenylsilane).[21,25,27] Using this equation and the data in Figure 12b yields rate constant ratios for mononuclear Ti-mediated copolymerizations (Table 8). The $k_p^{alkenylsilane}/k_{Si}^{total}$ rate constant ratios are all ≥ 1 and argue that chain transfer predominantly occurs subsequent to alkenylsilane enchainment. The alkenylsilane rate of insertion must be greater than the rate of total silane chain transfer to result in ratios ≥ 1, thus arguing that alkenylsilane enchainment occurs before the process of silane chain transfer. This explanation is in excellent agreement with the arguments advanced above to explain deviations from linearity in M_n vs $[alkenylsilane]^{-1}$ plots and the large LCB yields. In addition, as the alkenylsilane chain length decreases, the rate of alkenylsilane propagation becomes more competitive with ethylene propagation, doubtless reflecting steric factors.

Further evaluation of the role of the silane C=C functionality in the chain-transfer process was carried out with control polymerizations using saturated *n*-hexylsilane as the chain-transfer agent. ^1H NMR integration of SiH_2 versus vinyl resonances indicates the formation of predominantly vinyl-terminated polyethylenes, consistent with literature support for β-H elimination as the predominant chain-transfer process in ethylene + α-olefin copolymerization processes with these catalysts.[4b] Furthermore, the plot of M_n vs 1/[*n*-hexylsilane] reflects non-ideal chain transfer, with the near-zero slope indicating that $k_{Si}/k_p \approx 0$ (Figure 12d) and that silanolytic chain transfer is not the dominant termination pathway. In fact, alkenylsilanes are far more efficient chain-transfer agents than are alkylsilanes ($k_p^{ethylene}/k_{Si}^{total}$ for *n*-hexylsilane is up to 150 times greater than that of alkenylsilanes), indicating that the olefinic moiety is essential in alkenylsilane chain transfer. An appealing explanation is that the alkenylsilane chain-transfer rates are enhanced by high effective local silane concentrations achieved in proximity to the electrophilic Ti center, where the silyl group is held proximate to the Ti center either by insertion into the growing polymer chain (as argued above) or by interaction of the weakly basic silyl group with the Ti center[4c,d,17,28] (presumably via Scheme 2, steps iii and iv; less likely on the basis of the *n*-hexylsilane results). In addition, the olefinic moiety in the alkenylsilane may play a role by interacting with the electrophilic Ti center via olefin π-coordination,[28] also resulting in high effective local silane concentrations proximate to the active site.

$CGCTiMe_2$-mediated ethylene + 7-octenylsilane copolymerizations were conducted (Table 6, entries 1−7) with constant catalyst and monomer concentrations over a wide range of 7-octenylsilane concentrations (all in pseudo-zero-order excess). Interestingly, a superlinear relationship is observed between M_n and 1/[7-octenylsilane] (Figure 5), suggesting that the alkenylsilane length allows additional macromolecule-building chain-transfer processes beyond the conventional intermolecular Ti−polymeryl scission process (Scheme 3). Similarly, polymerizations with varying alkenylsilane concentrations (in pseudo-zero-order excess) were conducted using $EBICGCTi_2Me_4$ as the catalyst. That a sublinear relationship between M_n and 1/[alkenylsilane] is observed (Figures 3b and 4b) for alkenylsilanes ranging from C_3 to C_4 is consistent with the alkenylsilane acting as the dominant chain-transfer agent both inter- and intramolecularly at high [alkenylsilane]. In these systems, the LCB content compared to the total number of branches is approximately 10% and 20%, respectively, supporting the presence of both the inter- and intramolecular chain-transfer processes. Unlike the shorter alkenylsilanes, a superlinear relationship between M_n and 1/[alkenylsilane] is observed (Figures 1b and 5b) for alkenylsilanes of chain length C_6 and C_8. Here, high alkenylsilane concentrations produce high molecular weight polymer, most likely due to enhanced selectivity of presumably intradimer alkylsilane-branch chain transfer/macromolecule growing processes resulting in longer-chain branches (Scheme 3, step ii). In these systems, the LCB content compared to total number of branches is 25% and 20%, respectively, supporting the presence of the aforementioned chain transfer/macromolecule growing processes. These nonlinear systems are too kinetically

(27) [Ethylene] = 0.19 M. For ethylene solubility data in toluene, see: Wang, B. P. Ph.D. Dissertation, University of Massachusetts, 1989.

(28) Olefin interactions with d^0-metal complexes: (a) Stoebenau, E. J., III; Jordan, R. F. *J. Am. Chem. Soc.* **2006**, *128*, 8162. (b) Stoebenau, E. J., III; Jordan, R. F. *J. Am. Chem. Soc.* **2006**, *128*, 8638. (c) Carpentier, J.-F.; Maryin, V. P.; Luci, J.; Jordan, R. F. *J. Am. Chem. Soc.* **2001**, *123*, 898. (d) Casey, C. P.; Lee, T.-Y.; Tunge, J. A.; Carpenetti, D. W., II *J. Am. Chem. Soc.* **2001**, *123*, 10762. (e) Carpentier, J.-F.; Wu, Z.; Lee, C. W.; Stromberg, S.; Christopher, J. N.; Jordan, R. F. *J. Am. Chem. Soc.* **2000**, *122*, 7750. (f) Casey, C. P.; Carpenetti, D. W., II. *Organometallics* **2000**, *19*, 3970. (g) Casey, C. P.; Klein, J. F.; Fagan, M. A. *J. Am. Chem. Soc.* **2000**, *122*, 4320. (h) Casey, C. P.; Fisher, J. J. *Inorg. Chim. Acta* **1998**, *270*, 5. (i) Casey, C. P.; Hallenbeck, S. L.; Wright, J. M.; Landis, C. R. *J. Am. Chem. Soc.* **1997**, *119*, 9680. (j) Casey, C. P.; Hallenbeck, S. L.; Pollock, D. W.; Landis, C. R. *J. Am. Chem. Soc.* **1995**, *117*, 9770.

complex to analyze using eqs 6 and 7, mentioned above. In these nonlinear cases, multiple chain-transfer processes (Scheme 4) appear to be operative, including intermolecular transfer by alkenylsilane, intermolecular transfer by macromonomer silyl branches, intradimer transfer by silyl branches, and intramolecular cyclization by silyl branches. These silanolytic chain-transfer processes are far too multifaceted to be analytically tractable.

Conclusions

This investigation demonstrates that alkenylsilanes are versatile single-site comonomers having both the kinetic competence to efficiently effect silanolytic chain transfer in a variety of environments and the ability to undergo rapid insertive chain propagation. Moreover, the overall effectiveness of propagation for organotitanium-mediated copolymerizations with ethylene follows the order

$$C_8H_{15}SiH_3 < C_6H_{11}SiH_3 \approx C_4H_7SiH_3 < C_3H_5SiH_3$$

Smaller alkenylsilanes have more competitive propagation rates vs ethylene, as demonstrated by the large densities of short-chain branching in these systems. Longer alkenylsilanes have less competitive propagation rates compared to ethylene; however, the resulting polymers possess longer branches which subsequently undergo silanolytic chain transfer to other growing polymer chains, thus enhancing selectivity for long-chain branching. Furthermore, as the polymerization reaction time increases, the copolymer molecular weight linearly increases, suggesting long-chain branch formation via silane-branch chain transfer. Among the alkenylsilanes, 3-butenylsilane is the most efficient chain-transfer agent for $CGCTiMe_2$-mediated systems as a consequence of its moderate size. In addition, longer 7-octenylsilane is the most efficient chain-transfer agent for $EBICGCTi_2Me_4$-mediated copolymerizations as a consequence of its potential to contact other Ti−polymeryl moieties as well as to undergo facile intramolecular chain transfer with minimum ring strain in the resulting products. Allylsilane and 5-hexenylsilane are also found to be efficient chain-transfer agents for organotitanium-mediated polymerizations and produce substantial amounts of long-chain branching.

Several series of $CGCTiMe_2$-mediated polymerizations with varying alkenylsilane concentrations were examined and found to exhibit high polymerization activities, high product molecular weights, $M_w/M_n \approx 2.0$, negligible competing β-H elimination, and a linear relationship between M_n and 1/[alkenylsilane], all of which are consistent with a dominant silanolytic chain termination mechanism. Although the $EBICGCTi_2Me_4$-mediated polymerizations exhibit nonlinear relationships between M_n and 1/[alkenylsilane], these systems also exhibit high polymerization activities, high product molecular weights, $M_w/M_n \approx 2.0$, and negligible competing β-H elimination, consistent with a dominant, silanolytic chain termination mechanism. The ability to tune and modify the polyolefin microstructure (functional groups, long-chain branching) by varying the alkenylsilane chain length confers a great deal of flexibility on these polymerization systems. The versatility of these systems suggests the possibility of new and useful multipurpose comonomers for controlling polymer microstructure.

We have shown here that organotitanium-mediated silanolytic chain transfer and ethylene + α-olefin copolymerization can be coupled in a catalytic cycle to produce silane-terminated, highly branched copolymers with high propagation activities and narrow product molecular weight distributions. Therefore, introduction of alkenylsilanes into organotitanium-mediated ethylene polymerization systems is a versatile, effective new way of incorporating branches of various lengths and functionality into an otherwise inert polymer.

Acknowledgment. Financial support by the NSF (CHE-04157407) is gratefully acknowledged. We thank S. Shafaie and K. Gilmore for assistance with MALLS detector setup.

Supporting Information Available: Detailed experimental procedures and polymer characterization data (Figures S1−S4). This material is available free of charge via the Internet at http://pubs.acs.org.

JA0675292